NASA TECHNICAL
MEMORANDUM

INLET PLENUM CHAMBER NOISE MEASUREMENT
COMPARISON OF 20-INCH DIAMETER FAN
ROTORS WITH ASPECT RATIOS 3.6 AND 6.6

by Thomas F. Gelder and Richard F. Soltis

Lewis Research Center
Cleveland, Ohio 44135

1. Report No. NASA TM X-2191	2. Government Accession No.	3. Recipient's Catalog No.	
4. Title and Subtitle INLET PLENUM CHAMBER NOISE MEASUREMENT COMPARISON OF 20-INCH-DIAMETER FAN ROTORS WITH ASPECT RATIOS OF 3.6 AND 6.6		5. Report Date March 1971	
		6. Performing Organization Code	
7. Author(s) Thomas F. Gelder and Richard F. Soltis		8. Performing Organization Report No. E-5823	
9. Performing Organization Name and Address Lewis Research Center National Aeronautics and Space Administration Cleveland, Ohio 44135		10. Work Unit No. 720-03	
		11. Contract or Grant No.	
12. Sponsoring Agency Name and Address National Aeronautics and Space Administration Washington, D.C. 20546		13. Type of Report and Period Covered Technical Memorandum	
		14. Sponsoring Agency Code	

15. Supplementary Notes

16. Abstract

The effects of rotor blade aspect ratio, part-span damper design, and hub curvature on (1) blade passing-frequency noise, (2) multiple pure-tone noise, and (3) broadband noise from the inlet are presented for a wide range of speeds and airflow. Facility calibrations for noise are also discussed. Detailed radial aerodynamic measurements were also made. The higher aspect ratio reduced the noise level of blade passing frequency for all speeds; about a 9 dB reduction at 70-percent speed to about a 14 dB reduction at 100-percent speed. The reduced size of dampers along with reduced hub curvature greatly improved the aerodynamic performance of the rotor with little change in blade passing-frequency noise levels. The other two noise components were about the same for all rotors.

17. Key Words (Suggested by Author(s)) Engine noise Acoustics Compressors	18. Distribution Statement Unclassified - unlimited		
19. Security Classif. (of this report) Unclassified	20. Security Classif. (of this page) Unclassified	21. No. of Pages 49	22. Price* $3.00

CONTENTS

INLET PLENUM CHAMBER NOISE MEASUREMENT COMPARISON OF

20-INCH-DIAMETER FAN ROTORS WITH

ASPECT RATIOS OF 3.6 AND 6.6

by Thomas F. Gelder and Richard F. Soltis

Lewis Research Center

SUMMARY

Noise from three 20-inch (50.8-cm) diameter fan rotors was measured over a wide range of speeds and weight flow in a hard-wall inlet plenum chamber of an aerodynamic performance rig. Noise calibrations of the facility indicate that significant broadband and discrete-tone noise data were obtained although these data contain no directivity information, are for inlet only, and have not been verified by far-field measurements. Detailed radial aerodynamic measurements were also made. All rotors were designed for a total pressure ratio of 1.53 and a tip speed of 1150 feet per second (350 m/sec). Two of the rotors had different blade aspect ratios of 3.6 and 6.6 and corresponding blade numbers of 45 and 90. The third rotor was a modification of the 6.6-aspect-ratio rotor that reduced the size of its part span dampers and also reduced its hub curvature.

Blade passing frequency, multiple pure tones (also called combination tones), and broadband noise are compared with and also related to aerodynamic parameters. Fundamental blade passing-frequency sound pressure levels near peak aerodynamic efficiency operation were less for all speeds for the unmodified 6.6-aspect-ratio rotor than for the 3.6-aspect-ratio rotor - from about 9 decibels less at 70-percent speed to about 14 decibels less at 100-percent speed. The modified 6.6-aspect-ratio rotor had much improved aerodynamic performance over the original design with little change in blade passing-frequency noise levels. Multiple pure-tone noise levels were about the same for all rotors; also, the broadband noise levels did not vary much between rotors. The multiple pure tones became significant as soon as the tip relative Mach number exceeded about one, and then their combined sound pressure level had a higher value than single tones at blade passing frequency. At constant speeds, the broadband sound pressure levels continuously increased as the pressure ratio (or blade loading) was increased from near choke to near stall weight flow.

INTRODUCTION

Jet engine noise has been an increasing community problem, because of increasing thrust and frequency of flights, ever since jet-powered commercial service was introduced in the early 1950's. Recent air transport designs that emphasize economy and passenger comfort have introduced the use of high bypass ratio engines which require large fans. With such engines, fan noise dominates jet exhaust noise as illustrated by Kester and Slaiby (ref. 1). They also show the three noise components that are typically generated by transonic fans: (1) single pure tones at the blade passing frequency and its harmonics, (2) multiple pure tones, which occur at multiples of the frequency of shaft rotation, and (3) broadband noise. In the present study these three noise components were measured, and detailed radial aerodynamic measurements were also obtained for three transonic rotors (without stators). The rotor designs differed mainly in blade aspect ratio, part-span damper size, and hub curvature.

Fan noise generation depends on aerodynamic design and operation. This has been amply documented during the last decade, for example, in references 2 to 9. Unfortunately, detailed measurements of both noise and aerodynamic performance from the same tests, with realistic speeds and hardware, are not often found in the literature. One reason for this may be that best noise, or best aerodynamic, measurements are obtained from quite different test facilities. Also, some simplified scale model tests at subsonic speeds cannot simulate all the real noise sources and complexities of transonic fans. Typical outdoor noise test stands do not have the numerous, traversable, multi-parameter aerodynamic probes that indoor aerodynamic performance rigs have, and, in addition, they are subject to variable ambient conditions that could affect the data. On the other hand, typical indoor aerodynamic-performance rigs introduce some unnatural noise effects. One such effect results from hard reflecting walls enclosing a symmetrically shaped inlet plenum chamber. Such a chamber obscures the natural directivity of noise components and may even induce strong standing wave patterns for low-frequency tones. However, the possible benefits from noise measurements coupled with detailed aerodynamic measurements in an indoor aerodynamic performance rig are very attractive. These coupled results may identify cause and effect relations between noise and aerodynamic design and performance during the first phase of testing of advanced designs. With care, useful noise comparisons and trends from design changes should result from such indoor tests, especially if the tone noise is high frequency.

The purposes of the present study are (1) to examine noise components measured upstream of three fan rotors operated over a wide range of speed and flowrate in an indoor hard wall aerodynamic performance rig and (2) to compare noise components and aerodynamic performance from three rotors that differ mainly in blade aspect ratio, part-span damper size, and hub curvature. Emphasis is on the trends of and differences in each of the three noise components rather than on absolute sound power levels,

although these are also presented. Hopefully these and similar data where systematic design changes can be compared may help clarify the relations between noise generation and aerodynamic design so that noise reduction features may be properly assessed.

The 20-inch (50.8-cm) diameter rotors were designed for a pressure ratio of 1.53 and a tip speed of 1150 feet per second (350 m/sec). They had either 45 or 90 blades, corresponding to aspect ratios (ratio of mean span to axially projected chord at hub) of 3.6 or 6.6 and were tested without stators. The resulting fundamental blade passing frequencies at design speed were 10- or 20-kilohertz.

SYMBOLS

A_{an} minimum area of flow annulus for rotor absent tests, 1.34 ft^2 (0.125 m^2)

BPF   blade passing frequency

D diffusion factor, $1 - \dfrac{V_2'}{V_1'} + \dfrac{r_2 V_{\theta 2} - r_1 V_{\theta 1}}{(r_1 + r_2)\sigma V_1'}$

i_{ss} incidence angle to suction surface, angle between inlet-air direction and line tangent to blade suction surface at leading edge, deg

M Mach number

N rotor speed to design speed ratio

OASPL   overall sound pressure level, dB (referenced to 0.0002 microbar)

P total pressure, lbf/ft^2 (N/m^2)

p static pressure, lbf/ft^2

PWL   sound power level, dB (referenced to 10^{-13} W)

r radius, in. (cm)

SPL   sound pressure level, dB (referenced to 0.0002 microbar)

T total temperature, $^{\circ}$R (K)

V air velocity, ft/sec (m/sec)

v volume of plenum chamber (fig. 1), 470 ft^3 (13.3 m^3)

w weight flow, lbm/sec (kg/sec)

δ ratio of inlet total pressure to standard pressure of 2116 lbf/ft^2 (101 400 N/m^2)

δ^o deviation angle, angle between exit-air direction and tangent to blade mean camber line at trailing edge, deg

η adiabatic efficiency, $\dfrac{(P_2/P_1)^{\gamma-1/\gamma} - 1}{(T_2/T_1) - 1}$

θ ratio of inlet total temperature to standard temperature of 518.6^o R (288.1 K)

σ solidity of rotor blades, ratio of blade chord to spacing

τ reverberation time of plenum chamber, sec

$\bar{\omega}'$ rotor loss coefficient, $\dfrac{(P'_{2,id} - P'_2)}{(P'_1 - p_1)}$

Subscripts:

id   ideal

05   5-percent span from blade tip at trailing edge

1   station at rotor leading edge

2   station at rotor trailing edge

θ tangential direction

Superscript:

'   relative to moving blades

APPARATUS

Test Facility

The test facility for compressor and fan studies is shown by an overall drawing in figure 1(a) and by a detailed schematic of the region near the rotor in figure 1(b). Figure 1(b) shows the two rotor positions and the microphone locations that are used for the routine testing. The facility is sized for a maximum airflow rate of about 100 pounds per second (45.4 kg/sec). The air is usually drawn in from the roof of the building although laboratory refrigerated air is available. The air passes successively through turning vanes, a flow measuring orifice, another set of turning vanes, throttle valves, more turning vanes, and then into the 72-inch (183-cm) diameter plenum chamber. As shown by figure 1(b), the air then enters a 48-inch (122-cm) diameter pipe leading to a bellmouth which then reduces the flow path to the 20-inch (50.8-cm) diameter of the rotor tip. About 24 inches (61 cm) upstream of the rotors in a relatively low velocity

4

section are four support struts, equally spaced and airfoil shaped. Downstream of the rotor (fig. 1(a)) the air is turned into a toroid-shaped collector, then through another set of turning vanes and throttle valves to an altitude exhauster (although an atmospheric exhaust line is available). Outside air, altitude exhaust, and downstream throttling were used exclusively for the present tests.

A 15 000-horsepower (11 200-kW) synchronous motor drives the rotors. Variable-frequency equipment controls drive motor speed from 360 to 3600 rpm. With the gear-box used, a range of rotative speeds up to 17 500 rpm is available within an accuracy of ±0.2 percent.

The walls of the plenum chamber and all piping to and from it are rolled steel plate about 1/2-inch (1.3-cm) thick with no acoustic treatment anywhere. The volume of the chamber between the rotor and the first 90° bend upstream is about 470 cubic feet (13.3 m^3), and the corresponding wall surface area is about 388 square feet (36 m^2).

Rotors

The rotor blades used in these studies were machined from Maraging-200 steel bar stock. The blades are rigidly attached to a rotor disk; this assembly is hereafter referred to as a rotor. Rotor 1-mod 1 is shown in figure 2(a) by a front quarter-view photograph and in figure 2(b) by a side-view schematic drawing. Rotor 2 and rotor 2-mod 1 are similarly shown in figure 3(a) and (b). Rotor 1 is not shown because incomplete noise data were taken from it.

Table I summarizes the aerodynamic design values for the three rotors tested. To minimize blade vibrations, all rotors had plate type dampers that were located about one-third of the blade span from the tip (figs. 2(b) or 3(b)). One of the two differences between rotor 2 and rotor 2-mod 1 is that rotor 2-mod 1 had thinner and shorter damp-ers than rotor 2 (fig. 3(b)). The other difference between the two is that rotor 2-mod 1 has less hub curvature than that for rotor 2. The static tip clearance for all rotors averaged about 0.020 inch (0.050 cm).

Between the tests of rotor 2 and of rotor 2-mod 1 a facility change was made. This change, made for future stator and multistage tests, increased the axial space available between the inlet blade row and the collector. Thus rotor 2-mod 1 was mounted 15 inches (38 cm) upstream from where rotor 2 and rotor 1-mod 1 had been (fig. 1(b)).

Instrumentation

Aerodynamic. - Radially traversable probes were used to measure temperature, pressure, and air angle upstream and downstream of the rotor. These probes are

inserted through holes in the outer case at two circumferential locations and at two axial locations near the leading and trailing edges of the blades. Static pressure is measured by narrow wedge probes and also at the walls with flush taps. Total pressure, total temperature, and air angle are measured with a cobra type of combination probe (fig. 4).

Acoustic. - A schematic diagram of the acoustics instrumentation is presented in figure 5. A microphone calibrator of the pistonphone type was used with a 1/4-inch (0.64-cm) diameter condenser type of microphone. The microphone diaphragm was mounted perpendicular to the flow in the plenum chamber (fig. 1(b)). Three microphone locations were selected for routine testing based on noise calibration studies (described later). A remotely controlled traversing mechanism positioned the microphone in the plenum chamber to radii of 0, 18, and 26 inches (0, 45.7, and 66 cm) in an axial plane 108 inches (274 cm) upstream of rotor 1-mod 1 and rotor 2 or 93 inches (236 cm) upstream of rotor 2-mod 1.

The fractional-octave band analyzers (fig. 5) provide constant percentage bandwidths from 1 to 1/12 octave. The microphone signal was connected to either a 50-decibel range graphic level recorder, or a tape recorder, or both. The gain setting of the dc amplifier (fig. 5) was adjusted to optimize the voltage level of the signal for the tape recorder. Playback from the tape recorder is connected to either a (1) continuous constant bandwidth (3, 10, or 50 Hz) wave analyzer or (2) the fractional-octave analyzers previously described. Each analyzer is geared to its compatible graphic level recorder.

TYPICAL NOISE COMPONENTS UPSTREAM OF TRANSONIC FANS

Sound pressure level spectra from a fan rotor operating at subsonic- and supersonic-tip relative Mach numbers are shown in figure 6. Although the data of figure 6 are from an indoor hardwall facility they are similar to outdoor data (ref. 10). The continuous 50-hertz constant bandwidth spectra show three identifiable components of noise. The fundamental blade passing frequency at 8 kilohertz dominates the spectrum with subsonic-tip relative Mach numbers ($M'_{1,05}$ = 0.94; fig. 6(a)). In addition, a multitude of tones appear with frequencies less than the fundamental blade passing frequency when the tip relative Mach number becomes supersonic ($M'_{1,05}$ = 1.18; fig. 6(b)). The broadband level is generally 10 or more decibels below all the dominant tone levels in their frequency ranges.

The fundamental blade passing frequency and its harmonics for the rotor alone are primarily the result of the pressure distribution around each rotor blade. With uniform inflow, the lift and drag reaction forces on the air resulting from the blade pressure distribution are steady forces relative to the moving blade. However, at a fixed point on the rotor case, the rotating pressure field appears as an oscillating pressure. The frequency of the oscillation is the frequency with which a blade passes the fixed point or the

6

blade passing frequency.

The multiple pure tones (also called combination tones or supersonic fan noise) are the result of the shock-wave system associated with each rotor blade when the tip sections become supersonic. These are manifested forward of the fan by discrete tones but not at the blade passing frequency as ideal conditions would suggest. Instead, the wave system repeats itself each revolution of the rotor or shaft; thus the discrete tones can appear at all harmonics of rotor speed frequency. Reasons for this, as proposed in reference 11, are that the actual pressure wave forms are not identical blade to blade because of small manufacturing and assembly tolerances of rotor blades. According to reference 11, these can substantially affect the detailed shape of the wave system attached to each blade. Thus the real wave pattern at a distance from the blades repeats only once per revolution of the rotor or drive shaft. The highest levels of the multiple pure tones usually appear at frequencies below the fundamental blade passing frequency, and not all multiples of rotor frequency appear above the broadband noise level (fig. 6(b) and refs. 1, 10, and 11).

The third component, broadband noise, is the result of vortex shedding and possible turbulence in the approach stream. Vortices or eddies shed from the trailing edge can produce a sympathetic change in circulation, and hence lift force, on the blade surface. The multitude of different velocities, both chordwise and spanwise, results in a broadband of shedding frequencies. Also, tip vortexes are generated and shed and add to the broadband noise. Approach stream eddies or turbulence in the free stream or in the wall boundary layers can cause momentary fluctuations in rotor incidence angle and hence lift force. This random process also results in broadband noise.

A detailed review of the physics of broadband and periodic noise sources from rotating devices may be found in reference 12.

NOISE CALIBRATIONS AND DATA REDUCTION

This section is a detailed account of facility calibrations and data reduction techniques investigated for these noise studies. Briefly summarized, the section indicates that significant broadband and discrete tone noise data were obtained although the data contain no directivity information and have not been verified by far-field measurements.

Reverberation Time

These times are useful in assessing the uniformity of noise levels within an enclosure and also in estimating sound power levels from the measured sound pressure levels. Standard procedures for determining reverberation time (ref. 13, pp. 155 to 159) were

used to obtain the plenum chamber values shown in figure 7 for a wide range of frequencies. A random noise generator, a band pass filter, and amplifiers were used with a circular array of speakers in the annulus just upstream of the rotor to generate a noise field. Contiguous bands of noise 2/3-octave wide were generated, in turn, over a range from 0, to 20 kilohertz. One-third octave analysis centered within the various 2/3-octave bands was used to trace the sound decay time on a graphic level recorder. From these traces, the time for the sound to decay 60 decibels from a steady-state level (definition of reverberation time) was determined. As show in figure 7, the reverberation times at two different locations in the plenum chamber gave essentially the same result, especially above 1 kilohertz which is the frequency range of interest for these studies. These reverberation times along with room volume and surface area can be combined to calculate a total room constant as shown in reference 13 (p. 241). The resulting room constant is less than 50 square feet (4.7 m^2) which indicates a reverberant field. This means sound pressure levels should be the same anywhere in the plenum chamber. Such uniformity of sound level is confirmed by other measurements described next.

Effects of Microphone Location

Typical effects on sound pressure level spectra of radial location within the plenum chamber, 108 inches (274 cm) upstream of the rotor (see fig. 1(b)) are shown for three different but fixed radii in figure 8(a). Radial effects on selected single-tone levels are also shown in figure 8(b) with the microphone slowly but continuously traversing the plenum diameter. The 50-hertz bandwidth spectra of a rotor operating with supersonic tip relative Mach numbers (fig. 8(a)) are within 3 decibels of one another at the 0-, 18-, and 26-inch (0-, 45.7-, and 66-cm) radial locations. The 26-inch (66-cm) radius divides the area normal to the flow in half, and the 18-inch (45.7-cm) radius further divides the inner half flow area into equal parts. Remote radial traverses to radii greater than 26 inches (66 cm) were not possible with available equipment.

The continuous radial traverses across the inner 52 inches (132 cm) of the 72-inch (183-cm) diameter plenum (fig. 8(b)) reveal no consistent radial patterns. The peak-to-peak variation in sound pressure level of these tones is 4 decibels or less, irrespective of the frequencies shown. The frequencies of these tones nearly cover the range of fundamental blade passing frequencies for rotor 1-mod 1 operation and are about one-half the comparable frequency values for rotors 2. As frequency increases, the shorter wave lengths improve the uniformity of tone sound pressure levels. Also, the sound level variations of figure 8 are partly due to the inherent unsteadiness of the noise source as discussed in the section Effects of Time. An estimate of overall accuracy of the noise data as a function of microphone radius is presented in the section Reproduci-

8

bility and Accuracy. In summary, strong standing wave patterns are not evident in the plenum chamber for the frequencies of interest in this study.

The variation of broadband sound pressure levels with microphone radius was less than 1 decibel (fig. 8(a)).

Microphone traverses were also made along the axis of the plenum chamber. No significant variations in sound pressure level of tones or of the broadband noise were found. These data confirm the reverberation time data (fig. 7) and the room constant in that a diffuse sound field exists within the plenum chamber.

Background Noise of Facility

A 1/3-octave analysis of the combined auxiliary systems noises inherent to the normal operation of the compressor facility is presented in figure 9. From noise measurements of each auxiliary system operating alone, these systems, in order of decreasing overall noise, are the test cell ceiling exhaust fans, drive motor cooling air fans, and the oil system. The total overall sound pressure level of all auxiliaries is about 99 decibels referenced to 0.0002 microbar (corresponds to a sound power level of about 100 dB referenced to 10^{-13} W) and all this noise occurs below about 1 kilohertz. The noise of the auxiliaries is too low to influence the rotor noise measurements as will be shown.

Another check on facility noise was to measure its value as typical flow rates were induced by the altitude exhaust system (fig. 1(a)) with the rotor removed. A blank disk replaced the rotor and a smooth flow path was created in its place. The effects of flow alone on noise are shown by overall sound pressure levels and sound power levels (calculations described in PROCEDURES section) in figure 10(a) and by a 1/3-octave spectrum analysis in figure 10(b). Overall sound pressure (or sound power) of figure 10(a) increases directly with the fifth power of corrected weight flow. This fifth-power dependence is about that expected for flow noise as discussed in reference 14. The minimum area of the flow annulus was 1.34 square feet (0.125 m^2) at about 2 inches (5.1 cm) downstream of the rotor (fig. 2). This area chokes at a flow of 66 pounds per second (30.0 kg/sec) (fig. 10(a)), and then the inlet sound pressure level drops sharply. The sound level reduction was 4 to 8 decibels with the annulus choked. This reduction is a measure of the flow noise contribution of the facility downstream of the rotor plane. As shown by figure 10(b), most of the downstream flow noise is at frequencies above about 500 hertz.

Effects of Aerodynamic Measurement Probes on Noise

The stems of all radially traversable aerodynamic measurement probes had diameters of 1/4-inch (0.64 cm). The effect on noise of inserting these probes to within

1/4-inch (0.64 cm) of the opposite wall are shown in figure 11. The rotor was first operated without any probes and at 70 percent speed. Then, four equally spaced probes were inserted 3/4-chord length downstream of the rotor. Finally, three more probes were added 3/4-chord length upstream of rotor. As might be expected, the upstream probes created more noise than the downstream ones, and the presence of either adversely affected all the noise components from the rotor. Thus when taking noise measurements all traversable probes were withdrawn from the flow path.

Effects of Analyzer Bandwidth

A graphic level recorder trace of sound pressure level from spectrum analysis of transonic fan noise looks considerably different depending on the bandwidth. The first general problem is to select a bandwidth narrow enough to reveal all the tone noises of interest but not so narrow as to make data reduction needlessly time consuming. One-third-octave, 50-hertz constant, and 10-hertz constant bandwidth analyses are compared in figure 12 with a transonic rotor noise source (rotor 1-mod 1 at 100-percent speed and peak overall efficiency). The 1/3-octave analysis shows the fundamental blade passing frequency at 10 kilohertz; however, the cause of the predominate noise between 2- and 4-kilohertz is not at all apparent. In contrast, the 50-hertz constant bandwidth analysis of figure 12(b) shows that the predominate noise is a cluster of multiple pure tones spaced at the rotor frequency. The frequency at which a point on the rotor or shaft passed a fixed point was 220 hertz at design speed. Therefore, a 50-hertz bandwidth can separate adjacent harmonic peaks at all speeds that produce these shock-wave-originated multiple pure tones. The 10-hertz constant bandwidth analysis in figure 12(c) reveals little more than the previous 50-hertz analysis. The combined sound pressure level of the multiple pure tones is less than a 1/2 decibel difference between the 10 and 50 hertz analysis. The broadband level between figure 12(b) and (c) is necessarily different by 7 decibels (= 10 log 50/10) because of the bandwidth change. The 50-hertz constant bandwidth analysis appears to be about right for evaluating the three noise components of the present rotor designs.

Effects of Time

The inherent unsteadiness in the sound pressure level of discrete tones from fans is well known, even at constant speed and with ideal outdoor conditions (e.g., fig. 17 of ref. 6). Therefore, a representative time average of tone sound pressure levels is sought for best results. In figure 13 are typical indoor rotor data showing the effects of time on the sound levels of discrete tones at four different frequencies. These cover the

range of interest. The frequency-dependent parts of figure 13 show 1-kilohertz sections of the continuous frequency-sweep records using a 50-hertz bandwidth and minimum available writing speed or maximum pen damping. The time dependent parts (fig. 13) show the sound level variation for 40 seconds of a 50-hertz bandwidth whose center frequency is tuned to the discrete tone indicated. One of the multiple pure tones at 2.22 kilohertz (fig. 13(a)) shows a peak-to-peak variation with time of almost 7 decibels. On the other hand, fundamental blade passing frequency tones from 5 to 18 kilohertz (fig. 13(b) to (d)) show about half that variation. Comparing the left side with the right side of figure 13 shows that the continuous frequency-sweep analyses and pen damping which were routinely used gave fundamental tone levels that were in excellent agreement with averages over a 30- to 40-second interval. Also, for a single one of the multiple pure tones (fig. 13(a)), routine analysis levels may deviate about 1 decibel from 30-second time averages. However the total energy in all of them, based on 30-second time averages, is generally less than 1 decibel from the total indicated by the continuous frequency-sweep analysis. Although less pen damping rates were tried on these data, which in turn allows shorter analysis time, the results were not as good a time average as those shown in figure 13. Therefore, maximum available pen damping (i.e., minimum writing speed) was selected for all noise data reduction. With this pen damping, tone levels are believed to be accurate time averages within less than 1 decibel, and broadband levels within a few tenths of 1 decibel.

Reproducibility and Accuracy

Several of the operating points for a rotor were repeated a few days later and the noise data from each run were compared. Typical data from such a comparison are shown in figure 14. These sound pressure level spectra are from rotor 1-mod 1 operating at 100-percent speed and near peak aerodynamic efficiency. The microphone location was the same for both runs. The level of fundamental blade passing frequency at 10 kilohertz is about 1 decibel different. The multiple pure tones from the repeat runs are very similar in frequency content and in individual tone levels. Also, the broadband level is about the same throughout the spectrum, especially so for the highest levels between 2- and 4-kilohertz. There was only a 1/2-decibel difference in overall sound pressure level (OASPL) between the runs.

A summary of the reproducibility of noise data for the three different operating conditions and the three different microphone radii generally used is presented in table II. The data in table II are for rotor 1-mod 1 operating at 100-percent speed, but the data are similar to those for the other rotors and speeds. This tabulation is partly the basis for estimating the accuracy of the sound pressure levels presented in the next paragraph.

From the routine frequency-sweep analysis, the fundamental blade passing-frequency levels (table II(a)) show a maximum difference between microphone locations of 2.6 decibels for operation near peak efficiency (third run). For this run, assuming that the radial average of 30-second time averages represents the true sound pressure level, a single radius routine analysis could deviate as much as 1.8 decibels and a two-radius routine analysis average could deviate as much as 0.7 decibel. These decibel variations apply as well to operation near stall. However, near wide open throttle, these decibel variations are about halved. From routine analysis, the reproducibility of a particular tone level is within ±1.0 decibel at a particular microphone location and within ±0.9 decibel for a two-radius average. When all known effects on accuracy of the fundamental blade passing-frequency levels are considered (such as ability to define and repeat the operating condition, obtaining representative time averages, tape recorder effects, paper shifts and ink trace interpretation, and other possible calibration irregularities), the estimated accuracy of a two-radius routine analysis average is ±1.5 decibel. This inaccuracy applies to all rotors and operating conditions except near wide open throttle operation, and there it is about ±1.0 decibel.

For the summation level of all the multiple pure tones (exclusive of the fundamental blade passing frequency), a single radius value was ±2.4 decibels from the average, but two-radii averages were reproducible within 0.9 decibel (see table II(b)). The estimated accuracy of a two-radius routine analysis average for the summation level of multiple pure tones is ±1.5 decibels when all known effects are considered.

For the broadband sound levels (table II(c)) the differences between a single radius value and a two-radius routine analysis average was 0.5 decibel or less. Thus, the estimated accuracy of broadband levels is ±1.0 decibel including all known effects.

PROCEDURES

Aerodynamic Data

With rotative speed stabilized, the downstream throttle valve (fig. 1(a)) was adjusted to the desired weight flow as measured by the upstream orifice plate. Then the aerodynamic probes traversed the diameter in turn from the outer wall to 11 different radial positions. At each radial position, aerodynamic data were taken and automatically recorded on paper tape. These data were later processed through a streamline analysis data reduction program on a high-speed computer.

Immediately following the radial traverses for aerodynamic data, all these probes were withdrawn from the flow path and the noise data were recorded before the operating condition was changed.

Noise Data

Sound pressure levels. - At the start of each day's operation the microphone diaphragm and protective grid were inspected and, when necessary, cleaned of dirt particles. Then a known absolute sound pressure level of 124 decibels (nominal) at 250 hertz was applied to the microphone by the pistonphone calibrator (fig. 5). This signal was recorded on the graphic level recorder and on the tape recorder. Generally about 2 minutes of data for each operating point and microphone location were recorded (FM-mode) with the tape running at $7\frac{1}{2}$ inches per second (19 cm/sec). Periodically, the tape recorder range and center frequencies were checked and adjusted to maintain its optimum performance. About one-half of all noise data were also graphically recorded live for later comparison with the playbacks from tape. These comparisons generally showed less than 1/2-decibel differences for all noise components and frequencies. Two microphone radii were usually used for each operating point. Each component of the noise data presented is an energy average of the radial positions used.

In analyzing the data from the tape, continuous sweep-frequency analysis with 50-hertz constant bandwidth and maximum pen damping was routinely used to transcribe all the noise data to a graphic record. A typical record is illustrated in figure 6. From such a noise trace the broadband level was first drawn in as shown and used to calculate the total broadband level from 177 to 22 400 hertz. Near-zero frequencies were excluded because of possible starting transients and electronic noise in the recorder system; and above 22.4 kilohertz, the broadband level is generally low and of little practical interest. Next, all discrete tones were corrected downward by the amount of broadband contribution (insignificant correction for tone levels $\geq$ 10 dB above the broadband). Finally, where multiple pure tones were present, the sound energies of each corrected tone level (exclusive of the blade passing frequency level) were added together to yield a total multiple tone level for each operating condition. It is this total or summation of multiple pure tones that is used for comparisons.

Although not presented in this report, overall sound pressure levels (OASPL) and contiguous 1/12-octave records were also obtained for most of these data.

Sound power levels. - Although sound pressure levels are measured with standard microphones, values of sound power levels are desired for basic comparisons that are independent of the test facility and distance from the noise source. Therefore, an estimate of sound power level was made for each of the three noise components from the measured sound pressure levels and the volume v and reverberation time τ of the plenum chamber. The following equation from reference 13 (p. 177), which is derived in detail in an appendix of reference 15, was used:

$$PWL = SPL + 10 \log v - 10 \log \tau - 19$$

The sound power level PWL is in decibels (referenced to 10^{-13} W), and the sound pressure level SPL is a radial space average value in decibels (referenced to 0.0002 μ bar). Plenum chamber volume v between the rotor leading edge and the turning vanes just upstream of the plenum chamber (fig. 1(a)) is 470 cubic feet (13.3 m^3). Reverberation times τ at the appropriate frequencies were from figure 7. Both sound pressure level and sound power level are presented for completeness in subsequent noise results.

RESULTS AND DISCUSSION

Aerodynamic Performance of Rotors

Overall performance of rotor 1-mod 1. - A map of total pressure ratio as a function of corrected (or equivalent) weight flow is presented in figure 15. Constant corrected speed lines, the stall line, and adiabatic efficiency contours are shown. Also indicated is a peak efficiency line running through all speeds. (The speed lines shown are a well defined fairing of at least 10 different weight flows per speed.) The stall points were determined by slowly increasing the back pressure at constant speed (by throttling the flow) until a rapid fluctuation was noted in the signal from a hot-film gage. This gage was located near the rotor leading edge and outer case. The flow was then reset about 1 pound per second (0.45 kg/sec) higher, and steady-state data were recorded. The labelled stall line in figure 15 is drawn through these steady-state data points although stall flow is really 1 pound per second (0.45 kg/sec) lower.

Overall, the performance of rotor 1-mod 1 is good and near design values. For example, at design speed and flow, the actual pressure ratio was 1.51 compared with a design value of 1.53. The measured efficiency at design flow was about 89 percent compared with a design value of 92 percent (table I). The measured peak efficiency, near 91 percent, occurs at 60-, 80-, and 90-percent speeds. There is a very good flow margin of about 25 percent between the peak efficiency line and the stall line.

Blade-element performance of rotor 1-mod 1. - Radial distributions of several blade element parameters are presented in figure 16 for design speed at four different flows between choke and stall. Compared with the design values (dashed line), the losses $\bar{\omega}'$ and deviation angles δ^o are very high in the region of the vibration damper at a 68-percent span from the hub. Losses and deviation are especially high at the extremes of weight flow, either near stall (57.7 lbm/sec or 26.2 kg/sec) or near choke (76.7 lbm/sec or 34.8 kg/sec). Near design flow (74.2 lbm/sec or 33.6 kg/sec) incidence angles i_{ss} are near design over the outer half span but range up to 4° high near the hub. Consequently, losses near the hub are up somewhat from design values. Blade loadings as indicated by the diffusion factor D are near design values at design flow

operation. The radial distribution of relative Mach number M' matches the design values. The relative Mach number at a 5-percent span from the tip $M'_{1,05}$ is the independent variable selected for subsequent noise data plots.

Overall performance of rotor 2 and rotor 2-mod 1. - A performance map for rotor 2 is shown in figure 17(a), and a map for rotor 2-mod 1 in figure 17(b). Rotor 2 performance is far below design values of overall total pressure ratio (1.53) and efficiency (0.89). Also, rotor 2 performance was inferior to that of rotor 1-mod 1 (see fig. 16), although both rotors were designed to nearly the same specifications (see table I). The poor performance of rotor 2 prompted its modification. As shown in the section on blade element performance, losses in the hub region and in the damper region of rotor 2 were much higher than design values, even near design flow. Therefore, rotor 2 was modified by reducing hub curvature and reducing damper size as shown in figure 3(b). The overall performance of rotor 2-mod 1 (fig. 17(b)) was much improved over rotor 2 in both pressure ratio and efficiency. The performance of rotor 2-mod 1 is almost as good as rotor 1-mod 1. No detailed low-speed aerodynamic data were obtained with rotor 2-mod 1 although noise data were obtained at all speeds. There was an error in the recording of the low-speed aerodynamic data that was not discovered in time to rerun it. By then, a rotor blade had broken off near the damper. Whether the reduced damper geometry caused or contributed to the failure is not known.

Blade element performance of rotor 2 and rotor 2-mod 1. - The radial distributions of blade element parameters for rotor 2 and rotor 2-mod 1 are presented in figures 18 and 19 respectively. Only design speed and flows near peak efficiency are shown. The overall performance of rotor 2 was poor, as previously indicated, and figure 18 shows why. Hub deviation angles and hub losses are very high, suggesting a stalled hub region. Also the losses in the vicinity of the dampers were very high. As shown by figure 19, the reduced hub curvature modification to rotor 2 was effective in reducing deviation angles and losses in that region by reducing incidence angles there. In addition, thinning and shortening dampers (fig. 3(b)) greatly reduced the flow deviations and losses in that region.

Inlet Noise Performance of Rotors

Typical effects. - Before the levels of each of the noise components are summarized in detail, three typical effects on the noise spectra are discussed. These are the effects of throttle position at constant speed (blade loading), number of rotor blades, and an inlet lip disturbance during the testing of rotor 2-mod 1.

(1) Throttle position: Narrow band sound pressure level spectra at design speed for rotor 1-mod 1 at three different throttle positions are shown in figure 20. The

spectra are similar over a range between wide open flow at 75.8 pounds per second (34.7 kg/sec) (fig. 20(a)) and a flow between peak efficiency and stall at 68.0 pounds per second (30.9 kg/sec) (fig. 20(c)) in that the multiple pure tones and the fundamental blade passing frequency are easily identified and protrude above the broadband by 5 to 20 decibels. The broadband level increases steadily as the throttle is closed but the multiple pure tone content is somewhat less at the lowest flow shown. The noise levels of the fundamental blade passing frequency are similar although their adjacent frequencies have higher levels as the throttle is closed. Generally, noise data were not obtained in a stalled condition because of possible mechanical damage to the rotor and the facility. All subsequent noise data are from records similar to figure 20 where levels of the various noise components change only moderately with throttle position but not always in a predictable manner.

(2) Number of rotor blades: The fundamental blade passing frequency is a direct function of the number of rotor blades and shaft rpm. On the other hand, the revolutions per second of the rotor, which is the frequency spacing of multiple pure tones, is only a function of shaft rpm. Typical sound spectra for the 45-blade rotor (rotor 1-mod 1) and the 90-blade rotor (rotor 2) at design speed are shown in figures 21(a) and (b), respectively. For either rotor the multiple pure tones are similar and dominate the spectrum from about 2 to 5 kilohertz. The broadband noise levels are also similar. However at design speed, the fundamental blade passing frequency for rotor 1-mod 1 rises about 10 decibels above the adjacent broadband level, but with rotor 2 this tone, if present, is below the broadband level which itself is a few decibels less than for rotor 1-mod 1. But fundamental blade passing frequencies for rotor 2 are clearly present at speeds less than design, as shown by figure 22(a) for 80 percent of design speed. Reasons for the drastic difference in fundamental tone level between these rotors at design speed is not known. Relative velocities are the same for both.

(3) Inlet lip disturbance with rotor 2-mod 1: A facility modification, which was made after rotor 1-mod 1 and rotor 2 tests but before rotor 2-mod 1 tests, introduced a circumferential break in the surface of the inlet bellmouth. This discontinuity was at the downstream end of the bellmouth but ahead of the rotor leading edge (fig. 1(b)). A rotatable screen mechanism had been installed in this area for inlet flow distortion studies. This discontinuity, which was also connected to a small cavity under the flow surface, resulted in a stray tone near 2.7 kilohertz as shown in figure 22(b). Compared with rotor 2 at similar operating conditions (fig. 22(a)), the presence of the stray tone (the frequency of which did not vary with speed) is the only difference in the noise spectrums at 80 percent of design speed. The inlet lip discontinuity was not corrected in time to rerun the rotor 2-mod 1 noise data. Thus the multiple pure tone data of rotor 2-mod 1 is confused somewhat by the stray tone at 2.7 kilohertz. However, it was not a factor in determining either the broadband or the blade passing-frequency noise levels.

Summary of blade passing-frequency sound levels. - Blade passing-frequency sound
pressure and sound power levels for rotor 1-mod 1, rotor 2, and rotor 2-mod 1 are
presented in figure 23. The independent parameter selected is relative Mach number
at a 5-percent span from the inlet tip $M'_{1,05}$. Relative Mach number was also selected
as the one most pertinent for noise correlations in reference 6. At each of six rotation-
al speeds, three different throttle positions or blade loadings were set, and noise data
were recorded. The blade loadings at each speed are shown in the figures (see key) in
terms of an overall total pressure ratio P_2/P_1 and also in terms of a diffusion factor
at a 5-percent span from the tip D_{05}. With P_2/P_1 and the overall performance maps
(figs. 15 and 17), overall efficiency and weight flow are thus also available for each
noise data point. The selection of D_{05} is somewhat arbitrary. Perhaps the maximum
diffusion factor which tends to occur in the region of the damper (figs. 16 and 18) is
more appropriate. Presently, the tabulation of P_2/P_1 and D_{05} are intended for ref-
erence and are not used here for further correlation of the noise data.

The sound pressure levels shown (fig. 23) are generally an average of two different
radial positions of the microphone. The sound power levels are calculated as previous-
ly discussed and only differ from the sound pressure levels by a value that is within 2
decibels of a constant for all frequencies of interest. Therefore, noise trends and com-
parisons will be based on the measured sound pressure levels although they should apply
within a few decibels to the sound power levels as well. Also, in general, the level of
the fundamental blade passing frequency is at least 10 decibels above its next harmonic
for all rotors and speeds, except for rotor 1-mod 1 at low speeds. Here, the fundamen-
tal is either about 8 or about 5 decibels above the next harmonic at 60- or 50-percent
speed, respectively. Thus the sound levels of blade passing frequency shown in figure
23 are within about 1 decibel or less of the value of the fundamental frequency alone.
However, the harmonics were also analyzed and their levels included for rotor 1-mod 1
at low speed.

For rotor 1-mod 1 (fig. 23(a)) there is no consistent trend of blade passing-
frequency tone noise with loading at constant speed. The trend of this tone noise with
tip relative mach number $M'_{1,05}$ at a loading near peak efficiency is shown by a broken
line through solid symbols. Sound pressure increases directly with about the fifth power
of $M'_{1,05}$ up to a Mach number near 0.9, above which the tone noise level decreases.
Theory and experiment (ref. 6) indicate a sixth power variation with speed for blade
passing-frequency noise. The drop off in inlet sound levels at the higher speeds has
been observed by others (refs. 6 and 11). Although the absolute axial Mach number at
the rotor inlet is always subsonic, the maximum relative Mach number, which occurs
downstream of but near the leading edge, becomes supersonic over the outer span of
the blade. This occurs even with leading edge relative Mach numbers $M'_{1,05}$ of 0.9.
Thus, at least part of the noise generated on the rotor blade surface downstream of the

leading edge region may be choked off from propagating upstream.

Another feature about the blade passing-frequency levels for all rotors and all speeds tested is the propagation of all these tones into the plenum chamber. According to the so called cutoff theory, described by Tyler and Sofrin (ref. 16), rotor-only fundamental blade passing-frequency levels should decay exponentially whenever the tip speed is subsonic. According to reference 16, these decay rates would be about 40 and 80 decibels per axial inch for rotor 1-mod 1 and rotors 2, respectively. All rotor tip speed in figure 23 are subsonic, excepting the 100-percent speed data, and yet there is no apparent effect of operating below or through the cutoff speed. Propagation below cutoff has been observed and discussed by others (e.g., refs. 8 and 10). It seems to be the rule rather than the exception. Incoherence of the source and/or upstream turbulence could explain this contradiction of theory. Unfortunately, such nonideal features are typical of real machines and their environment.

For rotor 2 (fig. 23(b)) the level of blade passing frequency noise is down substantially from that of rotor 1-mod 1 at all speeds. For example, near peak efficiency loading, the blade passing-frequency levels for rotor 2 with a blade aspect ratio of 6.6 are about 9 decibels less at 70 percent speed to about 14 decibels less at 100 percent speed than those for rotor 1-mod 1 with a blade aspect ratio of 3.6. The rate of increase with speed below a $M'_{1,05}$ of 0.9 was also much less with rotor 2 than with rotor 1-mod 1. The fundamental blade passing frequency at design speed is 20 kilohertz for rotor 2 and 10 kilohertz for rotor 1-mod 1. However, for the distances and plenum conditions involved in these tests, there are insignificant variations in atmospheric attenuation between the 20- and 10-kilohertz frequencies. Also, the response of the 1/4-inch (0.64-cm) microphone used (fig. 5) is flat to frequencies well above 20 kilohertz. The reasons for this large reduction in blade passing-frequency levels with the higher aspect ratio blades are not presently known.

For rotor 2-mod 1 (fig. 23(c)) the levels of blade passing frequency noise at peak efficiency operation are about the same as for rotor 2 with the possible exception of 90- and 100-percent speed. Here, the blade passing frequency noise for rotor 2-mod 1 may be at least 3 decibels less than that for rotor 2. The modifications to rotor 2 that reduced the dampers and reduced the hub curvature did not change or even slightly lessened its noise. At the same time though, the aerodynamic performance was greatly improved to near design values as previously discussed (figs. 17 to 19). The unstalled hub and reduced damper losses of rotor 2-mod 1 were probably responsible for both the aerodynamic and blade passing-frequency noise improvement.

Summary of multiple pure-tone total sound levels. - Total multiple pure-tone sound pressure and sound power levels for rotor 1-mod 1 and both rotors 2 are presented in figure 24. The sound levels shown are a total (energy) of all apparent multiple pure tones exclusive of the fundamental blade passing frequency. As before, the different

18

blade loadings are tabulated and a dashed line is drawn through solid symbols to show peak efficiency operation. For reference, another dashed line shows the level of blade passing frequency near peak efficiency from figure 23.

For rotor 1-mod 1 (fig. 24(a)) multiple pure tones are not apparent below a relative tip Mach number of about 0.97. As this Mach number increases to supersonic values, the multiple pure-tone sound level increases sharply and is about 19 decibels above the level of the blade passing frequency at design speed. Although the level of the blade passing frequency decreases as $M'_{1.05}$ goes supersonic, the level of multiple pure tones does just the opposite. The multiple pure tone noise are not choked off with increasing Mach number because the source of this noise is the shock wave system itself. These trends are very similar to those shown in reference 11 for an 86-inch (218-cm) diameter fan demonstrator engine.

For rotor 2 and rotor 2-mod 1 (fig. 24(b)) the multiple pure-tone sound levels are about the same and are also not much different from those of rotor 1-mod 1. From the data of figure 24, it appears that for these rotors the relative Mach number is the most important parameter in determining the sound level of multiple pure tones, with blade loading having only secondary effects. For all rotors, the summation of multiple pure tones at peak aerodynamic efficiency points has a higher sound pressure or sound power level than single-tone levels at the blade passing frequency whenever the relative Mach number at the blade inlet tip exceeds about one. A similar crossover is shown in reference 11.

Summary of broadband sound levels. - The broadband sound pressure and sound power levels for rotor 1-mod 1, rotor 2, and rotor 2-mod 1 are presented in figure 25. A flow noise ceiling or maximum possible flow noise is also indicated by a dashed line for each rotational speed. This ceiling is from figure 10(a) at the same corrected weight flow. The dashed ceiling line is an attempt to separate that broadband noise caused by the rotor and its nearby ducting from that broadband noise caused by the facility ducts and valves which are not realistic simulations of rotor environment. The flow noise ceiling lines in figure 25 are believed to be at least 3 decibels too high for the situation with rotor present. This is because there was no inlet noise reducing effects because of baffling or reflection of downstream noise by the high solidity rotors in obtaining the flow noise data of figure 10(a). Figure 10(a) also indicates a maximum downstream flow noise increment of about 6 decibels from choking the annulus just aft of the rotor trailing edge. Thus we conclude that the broadband noise level data for all rotors (fig. 25) were not influenced by unrealistic noises from the facility for blade loadings near peak efficiency and higher. Only the wide open throttle data, that is, the highest relative Mach number data, at each speed, may be unrealistically high because of facility flow noise.

Broadband sound levels were less than 3 decibels different for all rotors at comparable operating conditions. Also, near peak efficiency operation, the broadband noise for all rotors varies directly with about the fifth power of tip relative Mach number. A sixth power variation is shown in references 3 and 6. For all rotors and speeds above 50 percent of design speed, the broadband sound levels at constant speed continuously increased as the pressure ratio or blade loading was increased from near choke to near stall weight flows. The increase in broadband noise level as stall incidence angle is approached was also noted in reference 3.

SUMMARY OF RESULTS

Noise from three 20-inch (50.8-cm) diameter fan rotors (no stators) was measured in a hard-wall inlet plenum chamber of an aerodynamic performance rig. Noise calibrations of the facility indicate that significant broadband and discrete-tone noise data were obtained although these data contain no directivity information, are for inlet only, and have not been verified by far-field measurements. The three rotors were designed for a pressure ratio of 1.53 and a tip speed of 1150 feet per second (350 m/sec). Two of the rotors had different blade aspect ratios of 3.6 and 6.6 and corresponding blade numbers of 45 and 90. The third rotor was a modification to the 6.6-aspect-ratio rotor that reduced the size of the part span damper and reduced its hub curvature. The following principal results were obtained:

1. Blade passing-frequency sound pressure levels or sound power levels near peak aerodynamic efficiency points were less for the unmodified 6.6-aspect-ratio rotor than for the 3.6-aspect-ratio rotor for all speeds: about 9 decibels less at 70 percent speed to about 14 decibels less at 100 percent speed. Modifications to the 6.6-aspect-ratio rotor that thinned and shortened its part-span damper and reduced its hub curvature greatly improved the aerodynamic performance of the rotor with little change in blade passing-frequency noise levels.

2. For all rotors, the summation of multiple pure tones (combination tones) has a higher sound pressure level or sound power level than single-tone levels at blade passing frequency whenever the relative Mach number at the blade inlet tip exceeds about one. Sound levels from the summation of multiple pure tones were about the same for all rotors when operating at the same tip relative Mach number.

3. Broadband sound pressure levels or sound power levels differed by less than 3 decibels for all rotors at comparable operating conditions. For all rotors and speeds above 50 percent of design speed, the broadband sound levels at a constant rotational

speed continuously increased as the overall pressure ratio or blade loading was increased from near choke to near stall weight flow.

Lewis Research Center,
    National Aeronautics and Space Administration,
        Cleveland, Ohio, October 12, 1970,
            720-03.

REFERENCES

1. Kester, J. D.; and Slaiby, T. G.: Designing the JT9D Engine to Meet Low Noise Requirements for Future Transports. Preprint 670331, SAE, April 1967.

2. Greatrex, F. B.: By-Pass Engine Noise. Preprint 162c, SAE, April 1960.

3. Sharland, I. J.: Sources of Noise in Axial Flow Fans. J. Sound Vib., Vol. 1, No. 3, 1964, pp. 302-322.

4. Bateman, D. A.; Chang, S. C.; Hulse, B. T.; and Large, J. B.: Compressor Noise Research, Tech Rept FAA-ADS-31, The Boeing Co., Commercial Airplane Div., Jan. 1965.

5. Hulse, B.; Pearson, C.; Abbona, M.; and Andersson, A.: Some Effects of Blade Characteristics on Compressor Noise Level. Tech Rept FAA-ADS-82, The Boeing Co., Oct. 1966.

6. Smith, M. J. T.; and House, M. E.: Internally Generated Noise from Gas Turbine Engines. Measurement and Prediction. Paper No. 66-GT/N-43, ASME, Mar., 1966.

7. Filleul, N. LeS.: An Investigation of Axial Flow Fan Noise. J. Sound Vib., Vol. 3, No. 2, Mar. 1966, pp. 147-165.

8. Lowson, M. V.: Reduction of Compressor Noise Radiation. J. Acoustical Soc. of America, vol. 43, no. 1, 1968, pp. 37-50.

9. Benzakein, M. J.; and Kazin, S. B.: Fan Compressor Noise Reduction. Paper No. 69-GT-9, ASME, Mar. 1969.

10. Goldstein, Arthur W.; Lucas, James G.; and Balombin, Joseph R.: Acoustic and Aerodynamic Performance of a 6-Foot-Diameter Fan for Turbofan Engines. Part II - Performance of QF-1 Fan in Nacelle Without Acoustic Suppression. NASA TN D-6080, 1970.

11. Kester, J. D.: Generation and Suppression of Combination Tone Noise from Turbofan Engines. In AGARD Conf. Procds. No. 42, Aircraft Engine Noise and Sonic Boom Conference, 1969, pp. 19-1-19-12.

12. Marte, J. E.; and Kurtz, D. W.: A Review of Aerodynamic Noise From Propellers, Rotors, and Lift Fans. Tech Rept 32-1462, Jet Propulsion Lab, Calif. Inst. of Technology, Jan 1, 1970.

13. Beranek, L. L., ed.: Noise Reduction. McGraw-Hill Book Co., Inc., 1960.

14. Harris, C. M., ed.: Handbook of Noise Control, McGraw-Hill Book Co., 1957.

15. Harley, K. G.; and Burdsall, E. A.: High Loading Low-Speed Fan Study, Part II. Data and Performance Unslotted Blades and Vanes. Rept. No. PWA-3653, Pratt and Whitney Aircraft, (NASA CR-72667), May 1970.

16. Tyler, J. M.; and Sofrin, T. G.: Axial Flow Compressor Noise Studies. SAE Trans., vol. 70, 1962, pp. 309-332.

TABLE I. - AERODYNAMIC DESIGN VALUES FOR ALL ROTORS

Tip diameter, in. (cm)	20 (50.8)
Tip speed, ft/sec (m/sec)	1150 (350)
Tip Mach no., $M'_{1,05}$	1.2
RPM	13 180
Pressure ratio, P_2/P_1	1.53
Solidity, chord/gap, σ_{05}	1.3
Blade shape	Double circular arc

Rotor	Aspect ratio	Number of blades	Chord length		Hub to tip radius ratio	Corrected flow, $w\sqrt{\theta}/\delta$		Tip diffusion factor, D_{05}	Overall efficiency, η
			in.	cm		lbm/sec	kg/sec		
Rotor 1-mod 1	3.6	45	1.82	4.62	0.4	73.9	33.5	0.38	0.92
Rotor 2	6.6	90	.93	2.36	.4	67.8	30.8	.40	.89
Rotor 2-mod 1	6.6	90	.93	2.36	.45	72.0	32.7	.44	.87

TABLE II. - TYPICAL REPRODUCIBILITY OF NOISE COMPONENTS FOR DIFFERENT OPERATING POINTS AND MICROPHONE RADII

[50 Hertz constant bandwidth analysis; rotor 1-mod 1; corrected speed, 100 percent of design.]

(a) Fundamental blade passing frequency

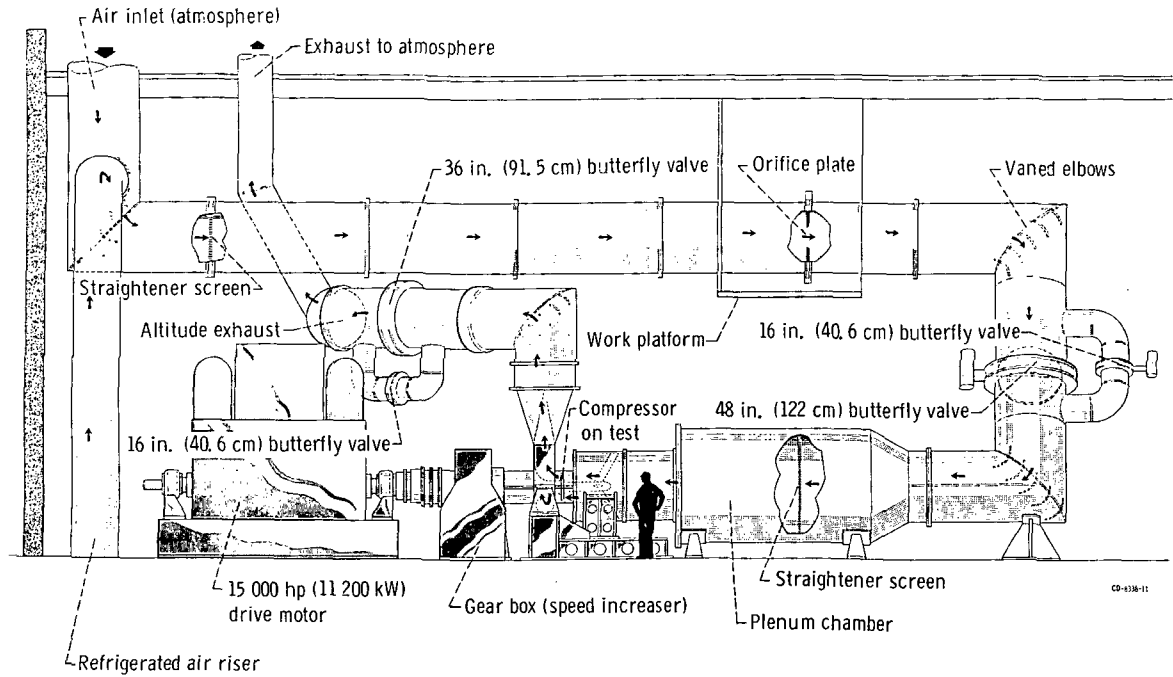| Microphone radius		Near peak efficiency				Near stall			Wide open throttle		
		First run	Second run (days later)	Third run (days later)	Average of repeat runs	First run	Second run (days later)	Average of repeat runs	First run	Second run (days later)	Average of repeat runs
in.	cm	Sound pressure level, dB[a]									
26	66.0	115.2	113.3	114.6	114.4±1.0	112.4	113.8	113.2±0.7	117.9	116.7	117.3±0.6
18	45.7	114.7	-----	-----	--------	-----	-----	--------	117.8	-----	--------
0	0	115.9	115.3	117.2	116.2±1.0	114.6	115.5	115.1±0.5	117.9	117.6	117.8±0.2
Radius average, routine		115.3±0.6	114.4±1.0	116.1±1.3	115.3±0.9	113.6±1.1	114.7±0.9	114.3±0.6	117.9±0.1	117.2±0.5	117.6±0.3
Radius average, over 30 sec		115.1±0.6	114.3±1.3	115.4±1.1	115.5±0.6	113.3±0.9	113.9±1.0	113.6±0.3	117.5±0.1	117.4±0.2	117.5±0.1

(b) Summation of multiple pure tones,[b] near peak efficiency

Microphone radius		First run	Third run (days later)	Average of repeat runs
in.	cm	Sound pressure level, dB[a]		
26	66.0	136.3	136.4	136.4±0.1
18	45.7	134.8	-----	--------
0	0	132.6	131.7	132.2±0.5
Radius average, routine		134.9±1.9	134.7±2.4	134.8±0.1

(c) Broadband, near peak efficiency

Microphone radius		First run	Third run (days later)	Average of repeat runs
in.	cm	Sound pressure level, dB[a]		
26	66.0	136.2	136.3	136.3±0.1
18	45.7	136.4	-----	--------
0	0	136.5	135.5	136.0±0.5
Radius average, routine		136.4±0.2	135.9±0.4	136.2±0.3

[a]Referenced to 0.0002 μbar.

[b]Blade passing tone excluded

Air inlet (atmosphere)

Exhaust to atmosphere

36 in. (91.5 cm) butterfly valve

Orifice plate

Vaned elbows

Straightener screen

Altitude exhaust

Work platform

16 in. (40.6 cm) butterfly valve

Compressor on test

48 in. (122 cm) butterfly valve

16 in. (40.6 cm) butterfly valve

15 000 hp (11 200 kW) drive motor

Gear box (speed increaser)

Straightener screen

Plenum chamber

Refrigerated air riser

(a) Overall view.

CD-8336-11

Rotor (20 (50.8) o.d.)

Screen (0.054 (0.137) diam wire, 50 percent open)

93 (236) for rotor 2-mod 1

Microphone locations (rotated 90° about centerline from actual)

26 (66)

18 (45.7)

48 (122)

72 (183)

Flow

24 (61)

120 (305)

Collector

108 (274) for rotor 1-mod 1 and rotor 2

(b) Rotor and microphone locations. (All dimensions are in inches (cm).)

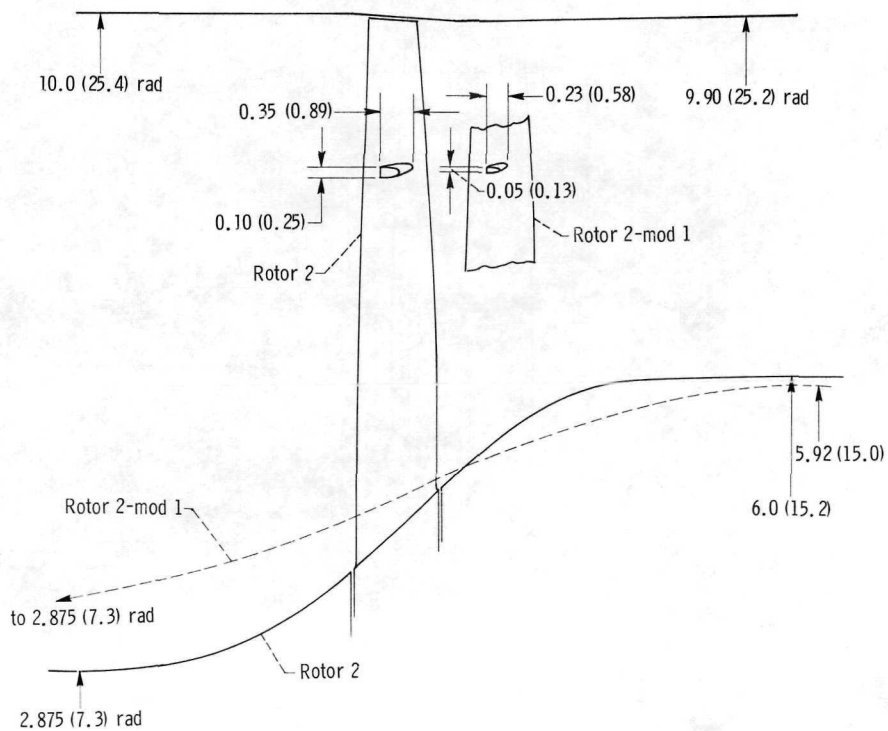Figure 1. - Compressor test facility.

24

(a) Front-quarter view

10.0 (25.4) rad

0.80 (2.03)

9.90 (25.2) rad

0.12 (0.30)

5.75 (14.6,

2.875 (7.3) rad
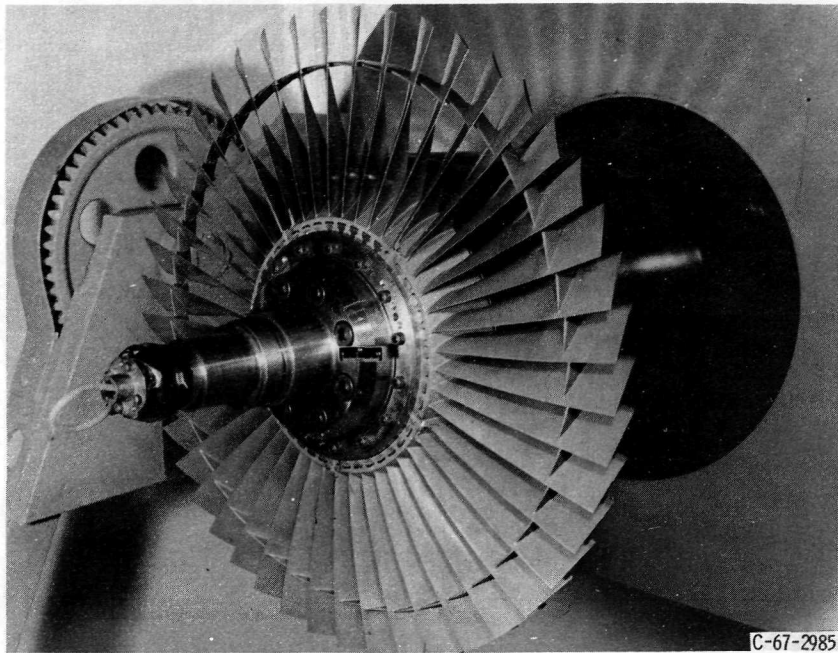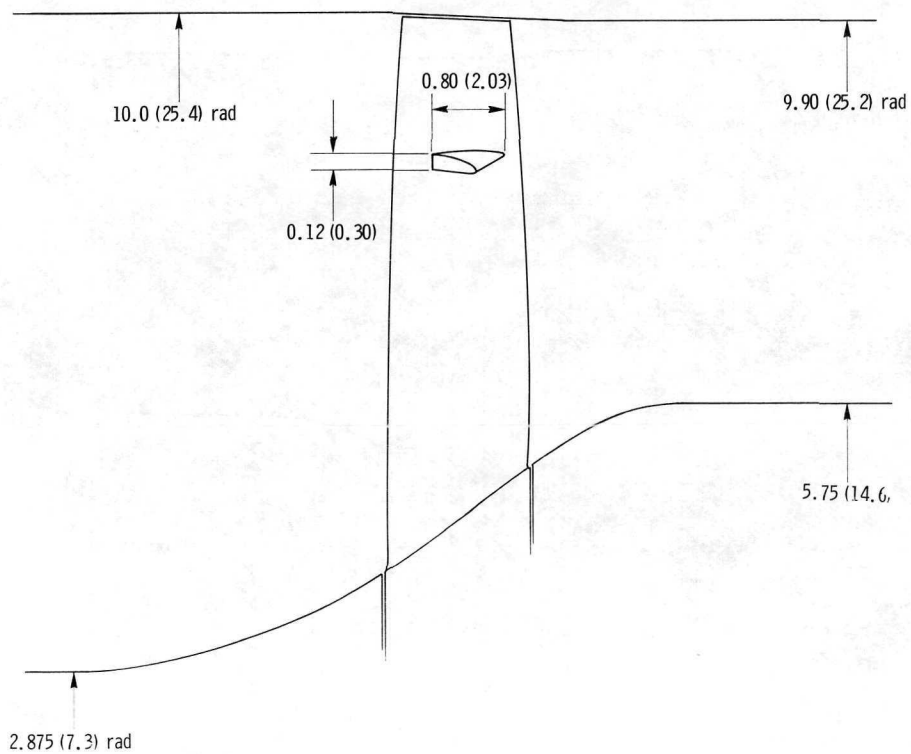
(b) Side-view schematic. (All dimensions are in inches (cm).)

Figure 2. - Rotor 1-mod 1.
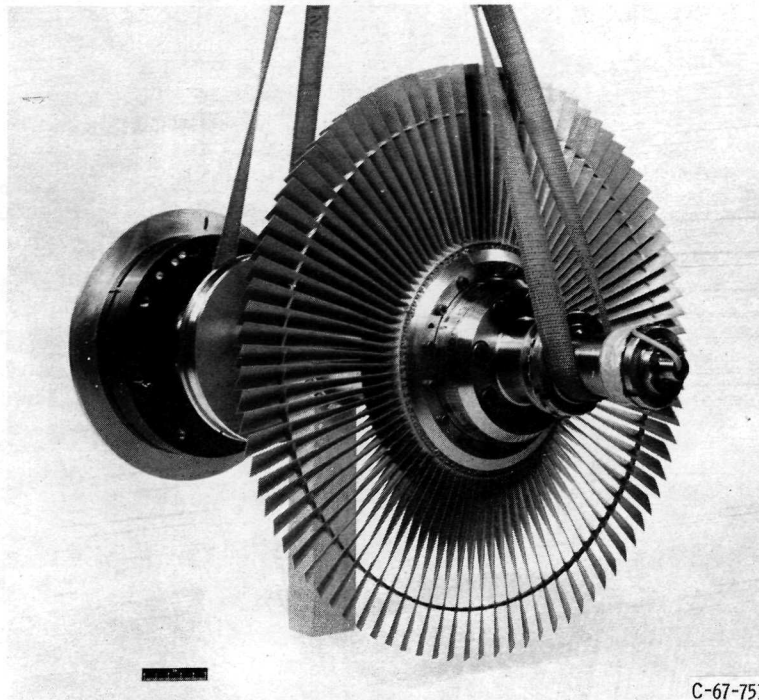
(a) Front-quarter view of rotor 2.

C-67-751

10.0 (25.4) rad

0.35 (0.89)

0.23 (0.58)

9.90 (25.2) rad

0.10 (0.25)

0.05 (0.13)

Rotor 2-mod 1

Rotor 2

Rotor 2-mod 1

5.92 (15.0)

6.0 (15.2)

to 2.875 (7.3) rad

Rotor 2

2.875 (7.3) rad

(b) Side-view schematic. (All dimensions are in inches (cm).)

Figure 3. - Rotor 2 and rotor 2-mod 1.

C-68-1281
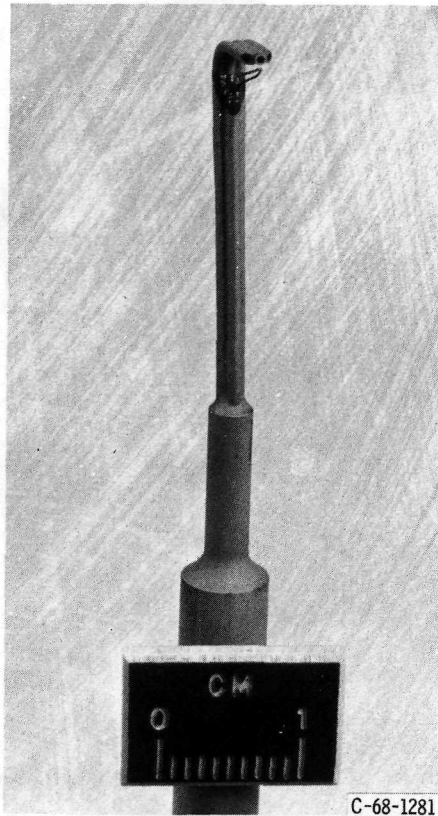
Figure 4. - Cobra-probe measures total pressure,
total temperature, and flow angle.

1. Bruel and Kjaer, type 4220
2. Bruel and Kjaer, type 4136
3. Bruel and Kjaer, type 2615
4. Bruel and Kjaer, type 2107
5. Bruel and Kjaer, type 1612
6. Dana
7. Bruel and Kjaer, type 2305
8. Consolidated Electrodynamics, type VR 3600
9. General Radio Co., type 1900-A
10. General Radio Co., type 1521-B

———————→ Live or direct
----◄--- Playback
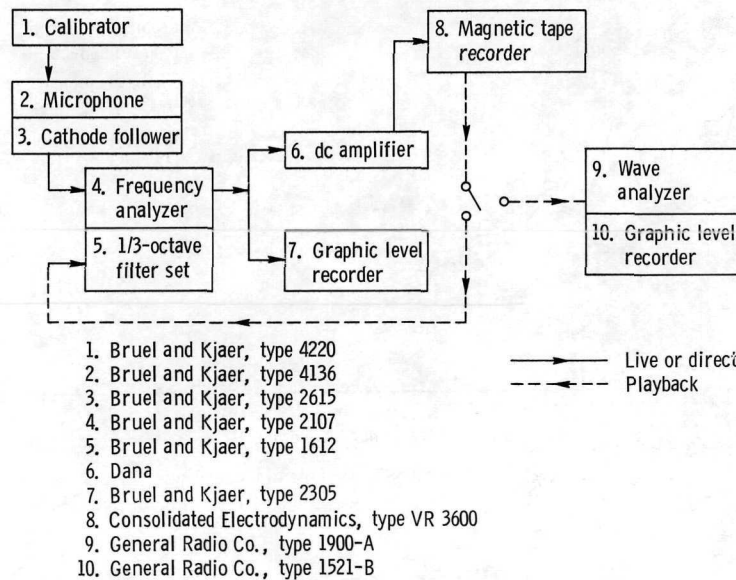
Figure 5. - Schematic diagram of acoustics equipment.

(a) Subsonic tip relative Mach number, 0.94; corrected speed, 80 percent of design.

(b) Supersonic tip relative Mach number, 1.18; corrected speed, 100 percent of design.
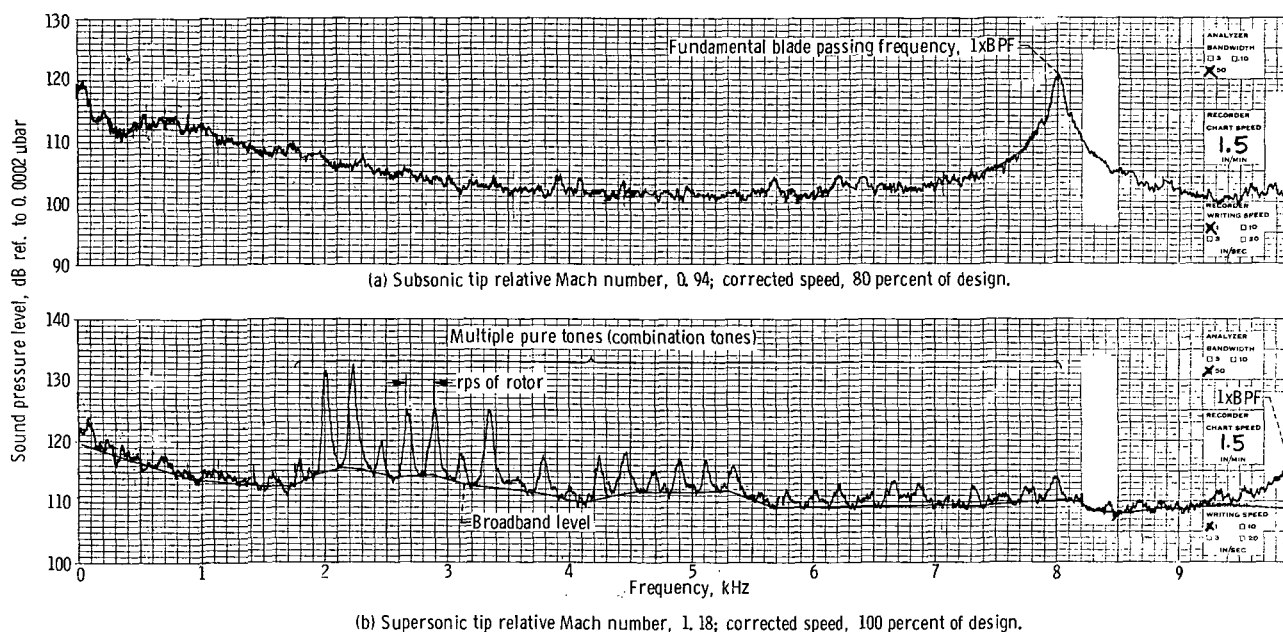
Figure 6. - Typical inlet sound pressure level spectrum; 50-hertz constant bandwidth analysis. Rotor 1-mod 1.
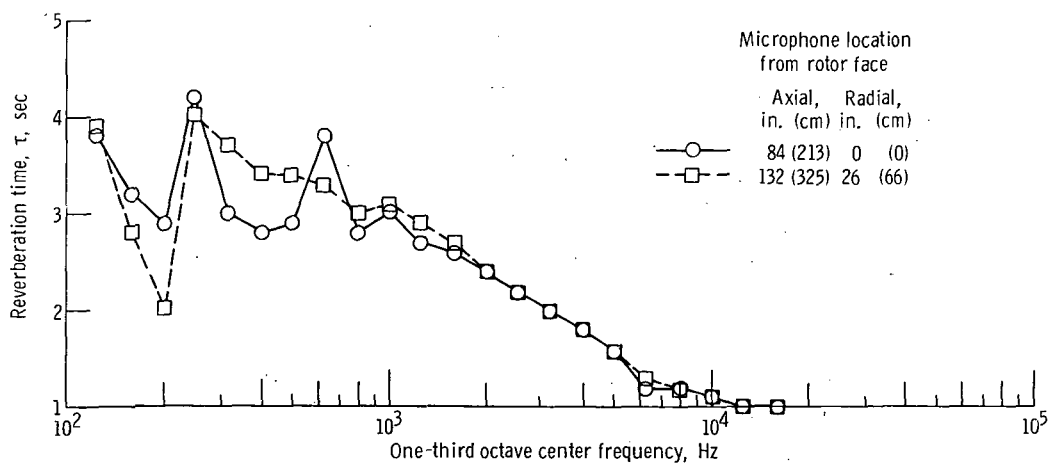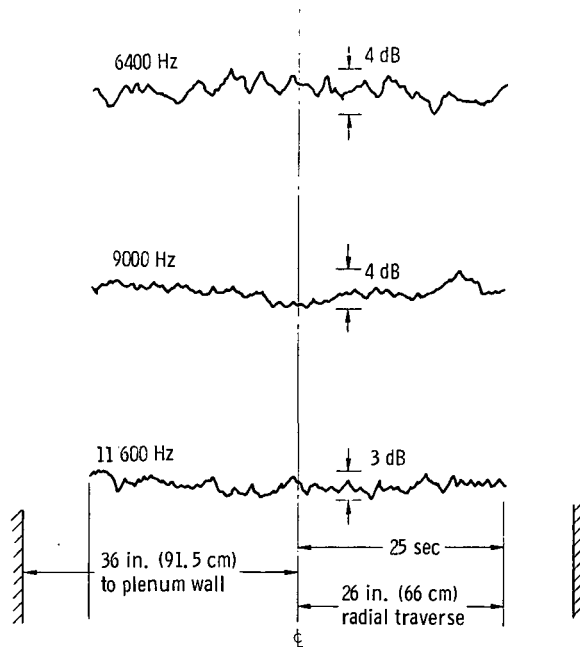

Figure 7. - Reverberation time of plenum chamber.

28
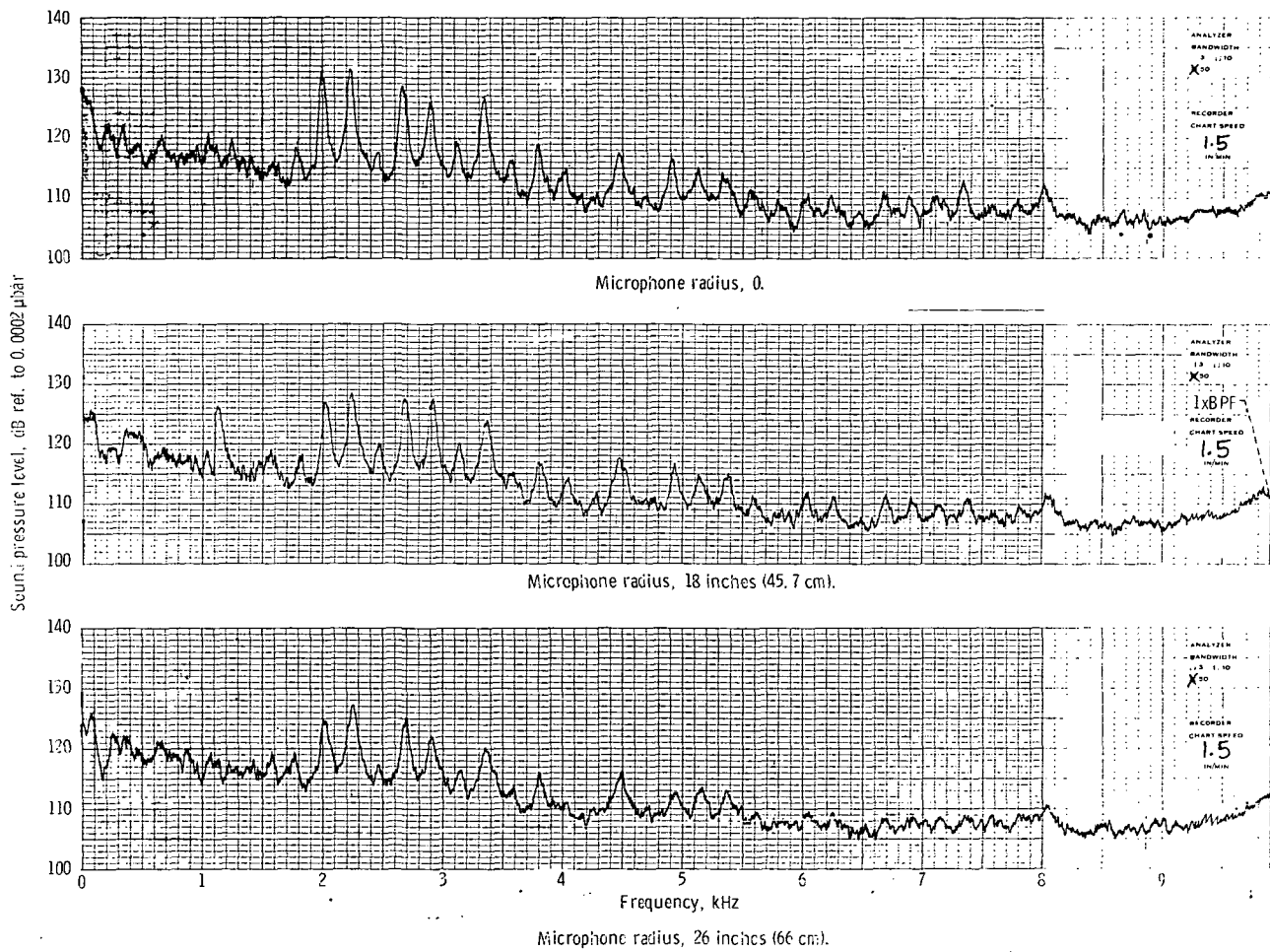
(a) Spectrum levels at three fixed microphone locations.

Figure 8. - Typical effects of radial location on 50-hertz bandwidth sound pressure levels in plenum chamber 108 inches (274 cm) upstream of rotor.

29

6400 Hz

4 dB

9000 Hz

4 dB

11 600 Hz

3 dB

36 in. (91.5 cm)
to plenum wall

25 sec

26 in. (66 cm)
radial traverse

¢

(b) Single tone levels as microphone continuously traverses.
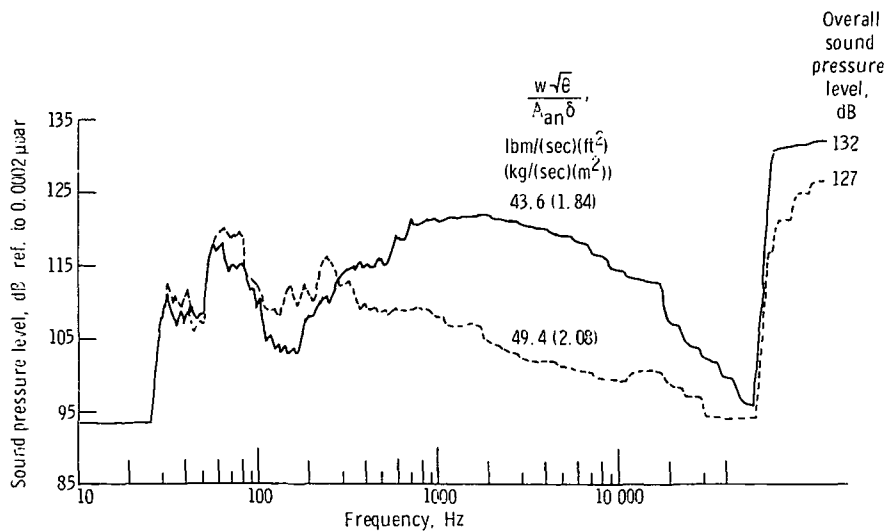
Figure 8. – Concluded.
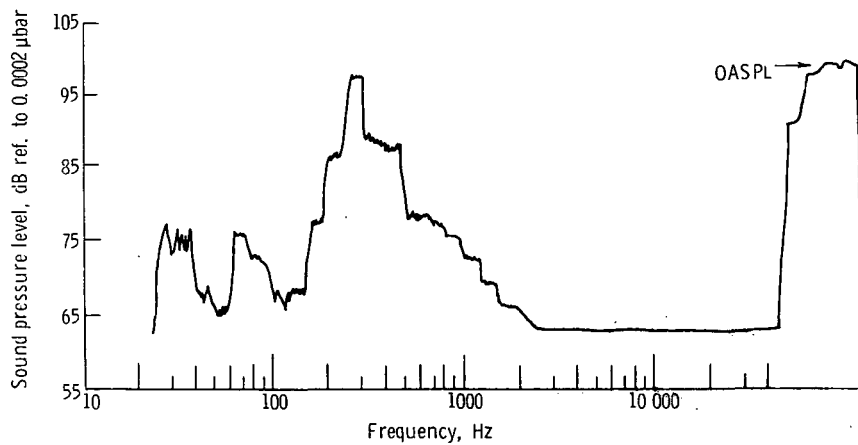
Figure 9. – Compressor test facility background noise of auxiliaries: room exhaust fans, drive
motor cooling fans, and oil system. Overall sound power level, 100 decibels (referenced to
10^{-13} W). One-third octave spectrum analysis.
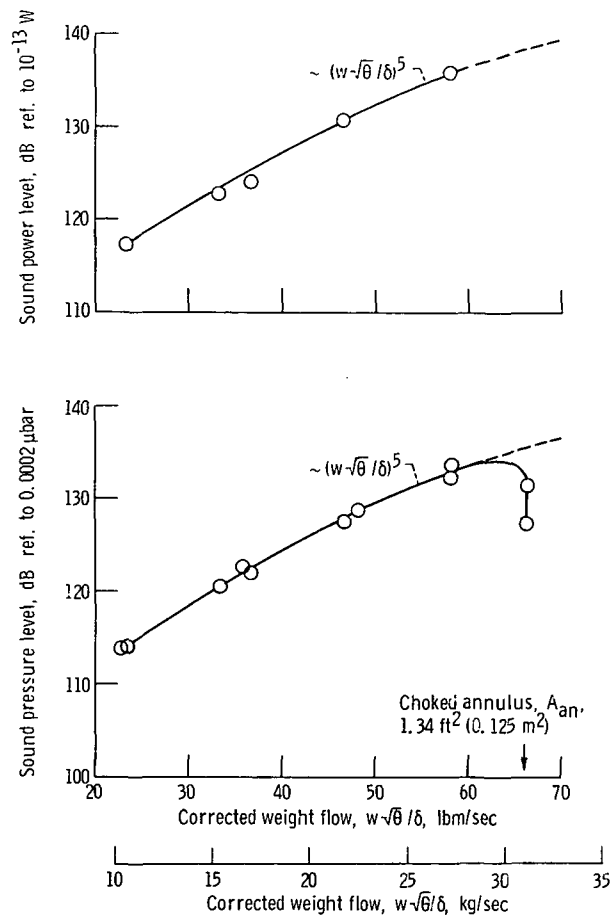
(a) Overall (177 to 22 900 Hz) sound pressure level and sound power level.

(b) One-third octave spectrum analysis at two flows, one of which chokes the annulus.

Figure 10. - Effects of corrected weight flow induced without rotor.
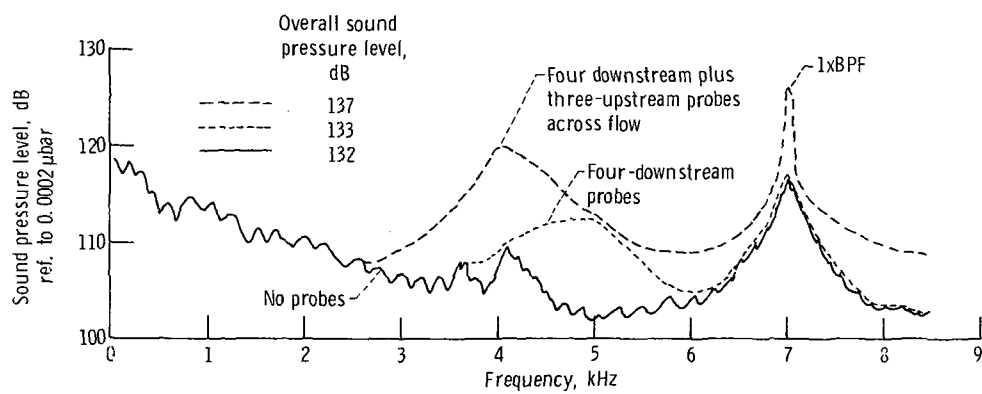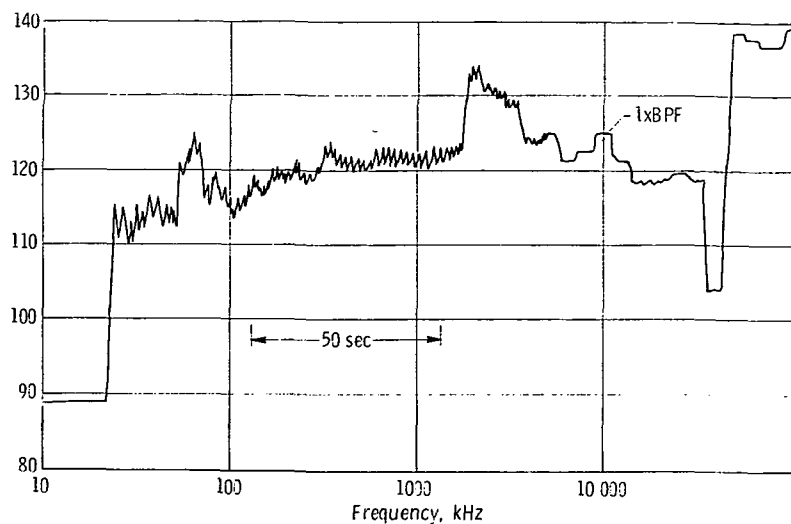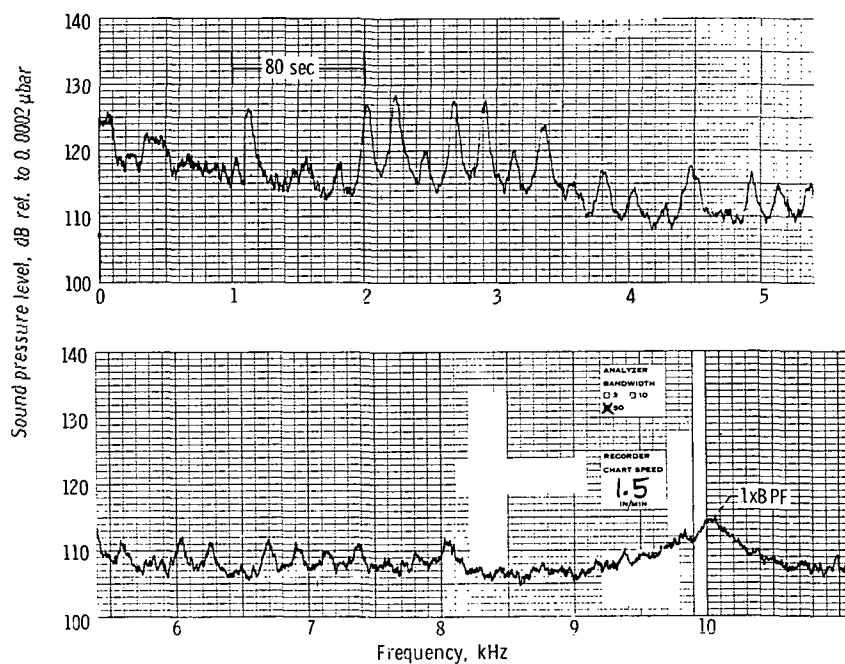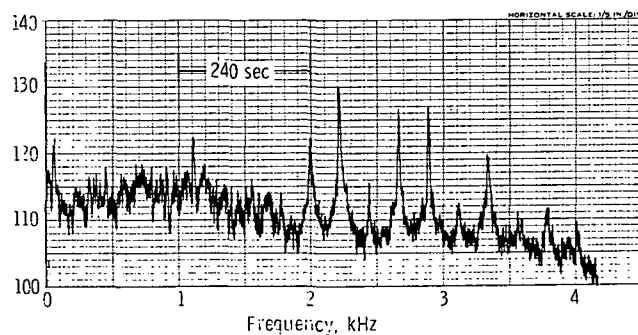
31

Figure 11. - Typical effects of aerodynamic measurement probes on sound pressure level spectrum, 50 hertz bandwidth; rotor 1; corrected speed, 70 percent of design.

(a) Bandwidth, one-third octave.

(b) Bandwidth, 50 hertz (constant).

(c) Bandwidth, 10-hertz (constant).

Figure 12. - Typical effects of analyzer bandwidth on sound pressure level spectrum.

(a) Multiple pure tones. Rotor 1-mod 1; corrected speed, 100 percent of design.

(b) Fundamental blade passing frequency. Rotor 1-mod 1; corrected speed, 50 percent of design.

(c) Fundamental blade passing frequency. Rotor 1-mod 1; corrected speed, 100 percent of design.

(d) Fundamental blade passing frequency. Rotor 2; corrected speed, 90 percent of design.
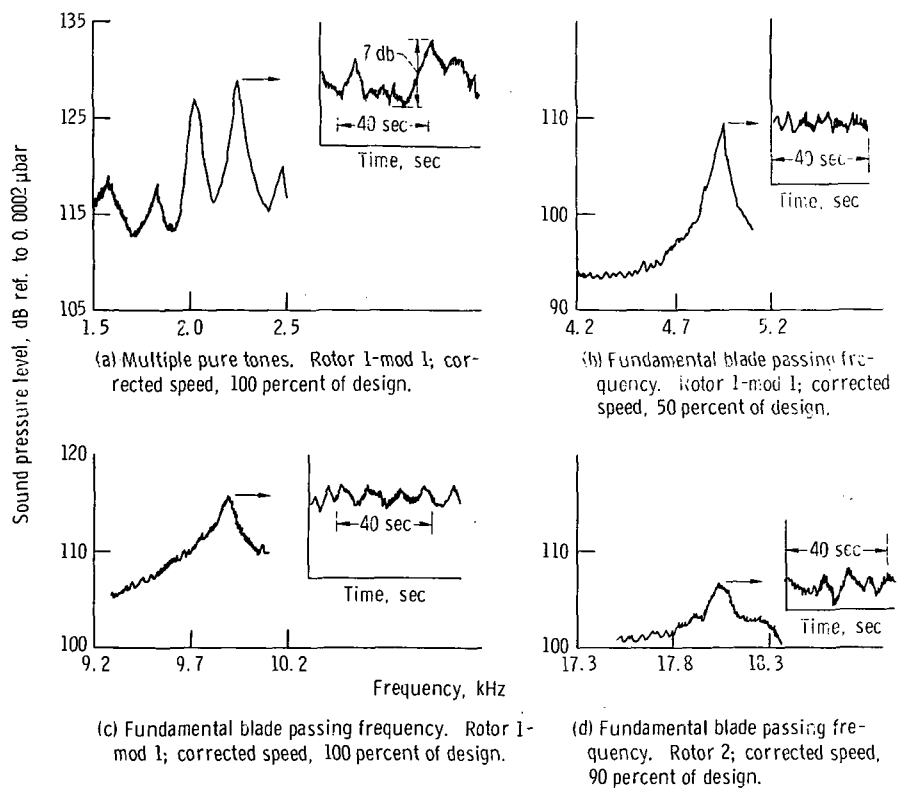
Figure 13. - Typical effects of time on sound pressure levels in 50-hertz bandwidths centered on various tone frequencies. Maximum pen damping.
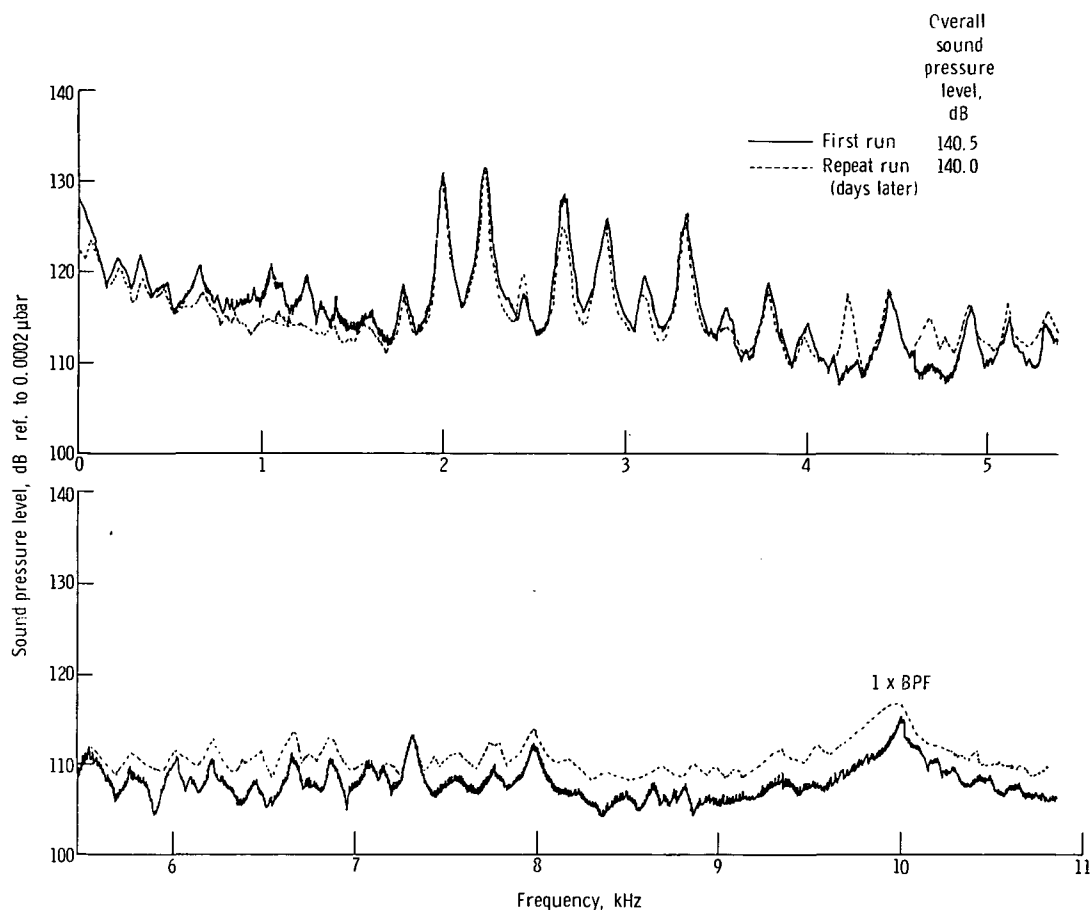
Figure 14. - Typical reproducibility of inlet sound pressure level spectrum. 50-Hertz bandwidth; rotor 1-mod 1 corrected speed, 100 percent of design; near peak aerodynamic efficiency.

Figure 15. - Overall aerodynamic perform-
ance of rotor 1-mod 1.
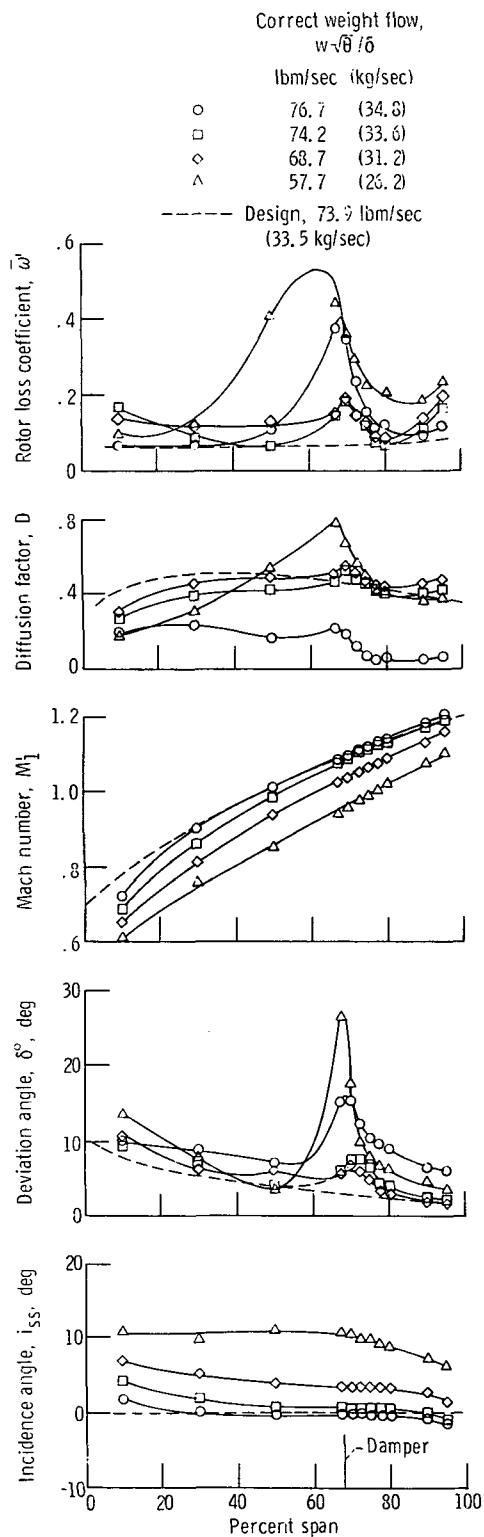
Figure 16. - Radial distribution of blade element parameters. Rotor 1-mod 1; corrected speed, 100 percent of design; various weight flows.
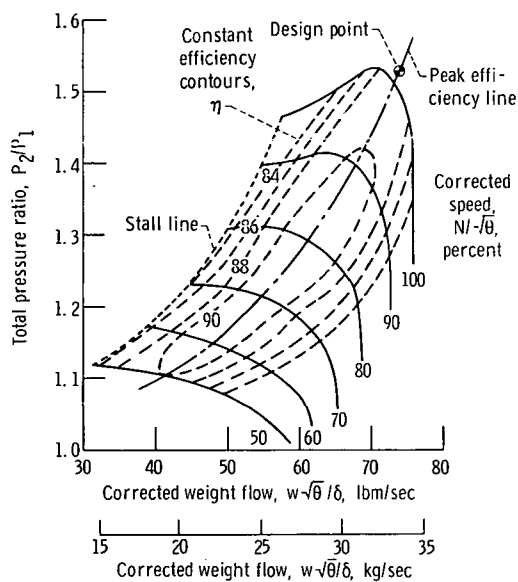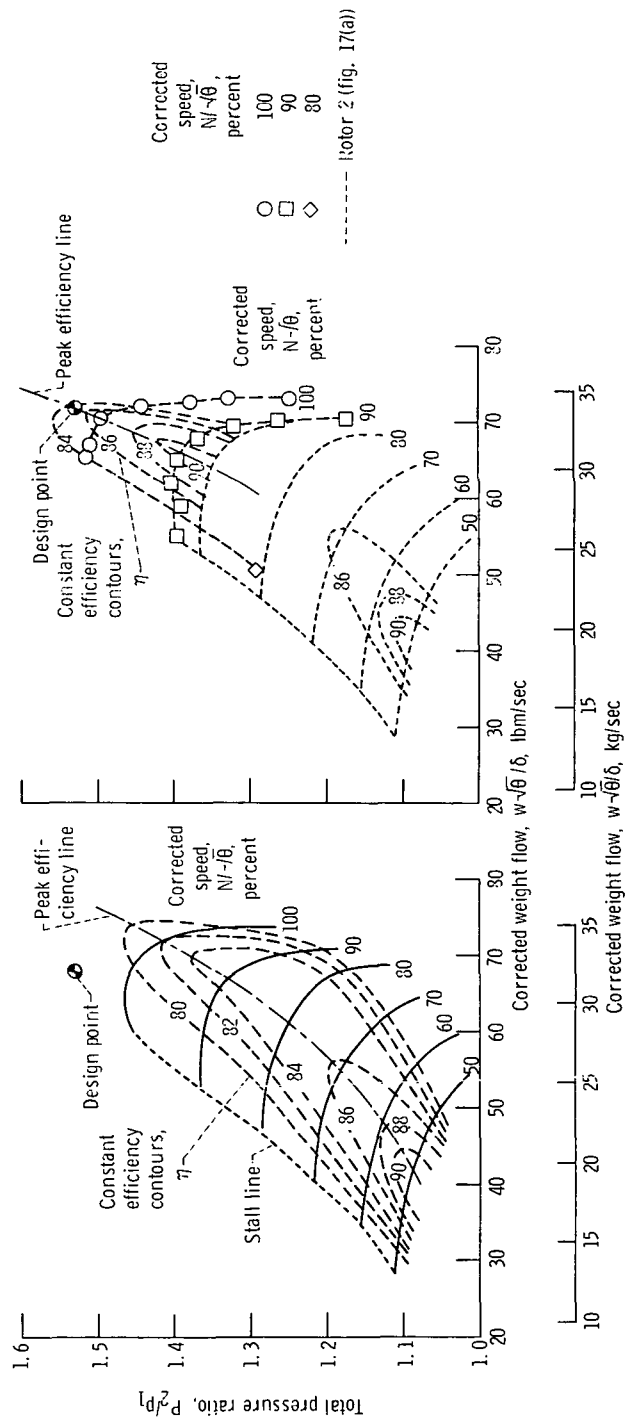
Figure 17. - Overall aerodynamic performance.

(a) Rotor 2.

(b) Rotor 2-mod 1.

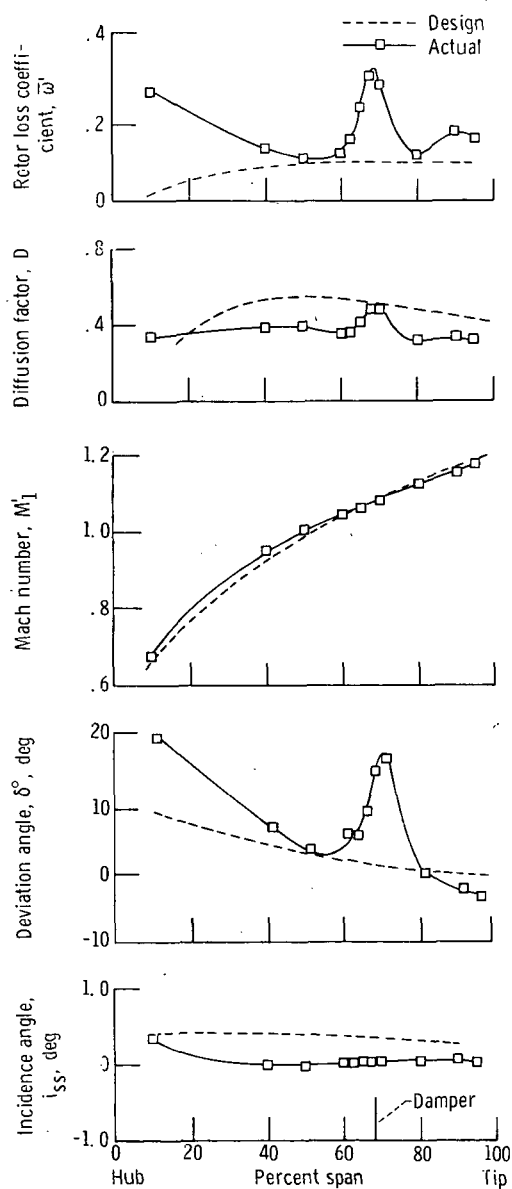Figure 18. - Radial distribution of blade-element parameters. Rotor 2; corrected weight flow, 71.6 pounds per second (32.5 kg/sec); corrected speed, 100 percent of design; near peak efficiency.
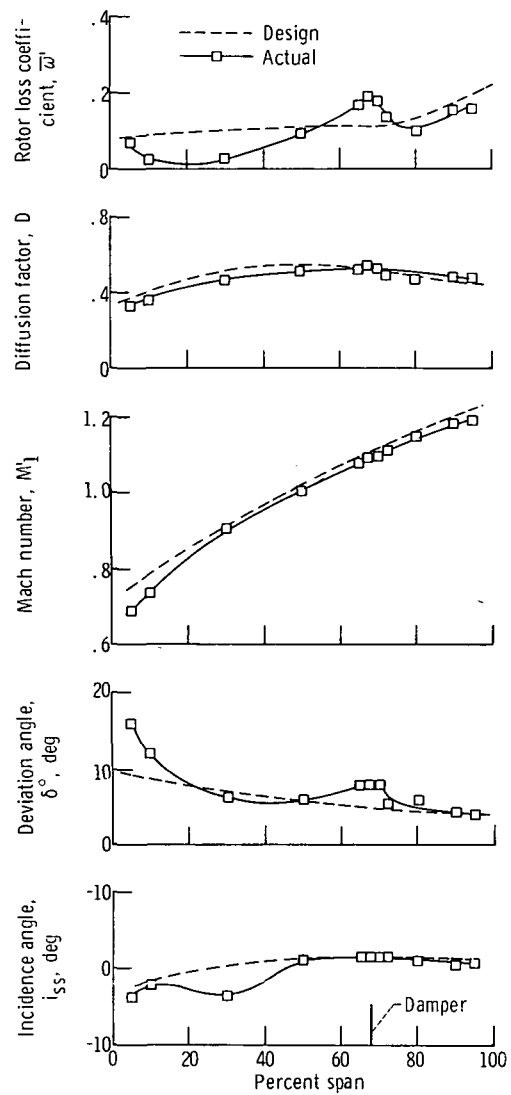
Figure 19. - Radial distribution of blade-
element parameters. Rotor 2-mod 1; cor-
rected weight flow, 70.8 pounds per second;
corrected speed, 100 percent of design; near
peak aerodynamic efficiency.

39

(a) Wide open throttle (choke); corrected weight flow, 75.8 pounds per second (34.4 kg/sec); total pressure ratio, 1.26; diffusion factor at 5-percent span, 0.36.

(b) Near peak efficiency; corrected weight flow, 73.4 pounds per second (33.3 kg/sec); total pressure ratio, 1.51; diffusion factor at 5-percent span, 0.43.

(c) Near stall; corrected weight flow, 68.0 pounds per second (30.9 kg/sec); total pressure ratio, 1.52; diffusion factor at 5-percent span, 0.48.

Figure 20. - Effect of throttle (weight flow and pressure ratio) on sound pressure level spectrums. Rotor 1-mod 1; corrected speed, 100 percent of design; microphone radius, 26 inches (66 cm).

Frequency, kHz

Sound pressure level, dB ref. to 0.0002 μbar

Sound pressure level, dB ref. to 0. 0002 μbar

Frequency, kHz

(a) Number of blades, 45; rotor 1-mod 1.

(b) Number of blades, 90; rotor 2.

Figure 21. - Effect of blade number on inlet sound pressure level spectrum. Corrected speed, 100 percent of design; near peak efficiency.

41

Figure 22. – Comparison of inlet sound pressure level spectrum for rotor 2 and rotor 2-mod 1. Corrected speed, 80 percent of design; near peak efficiency.
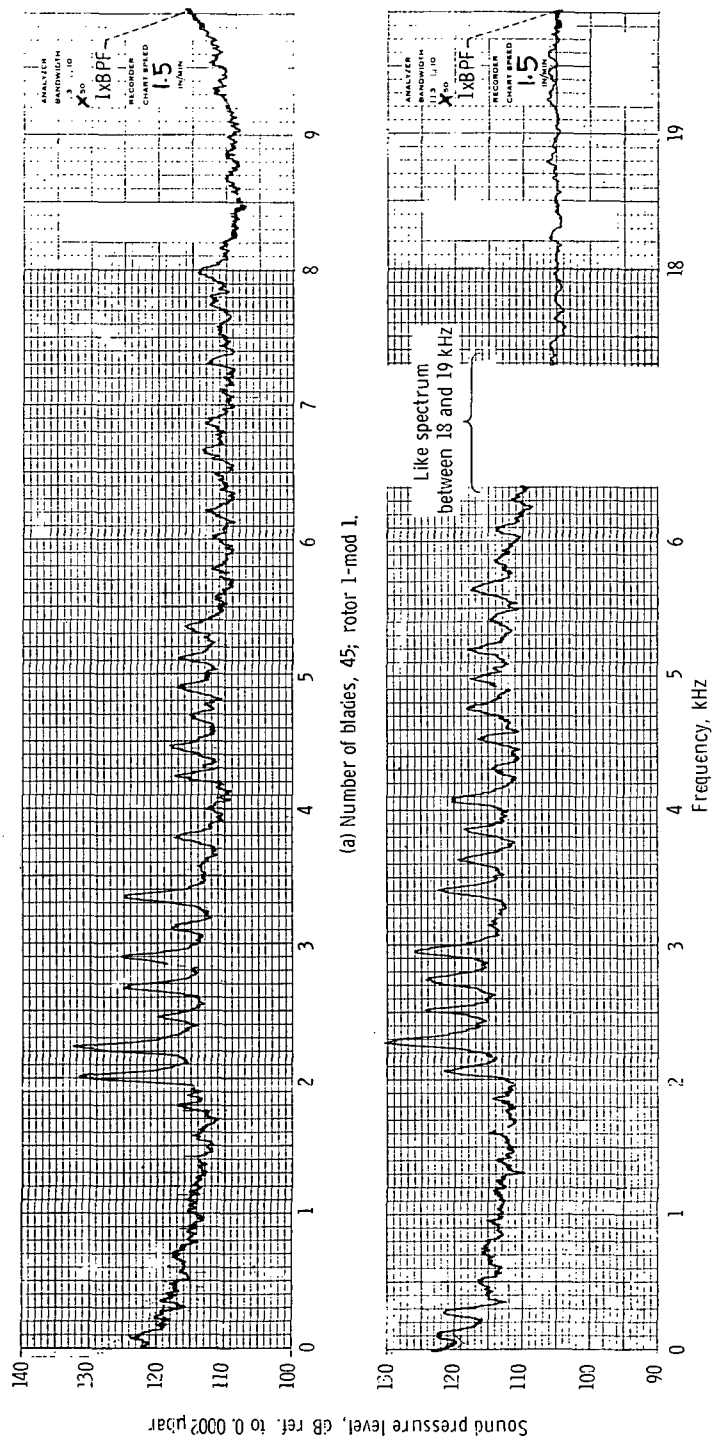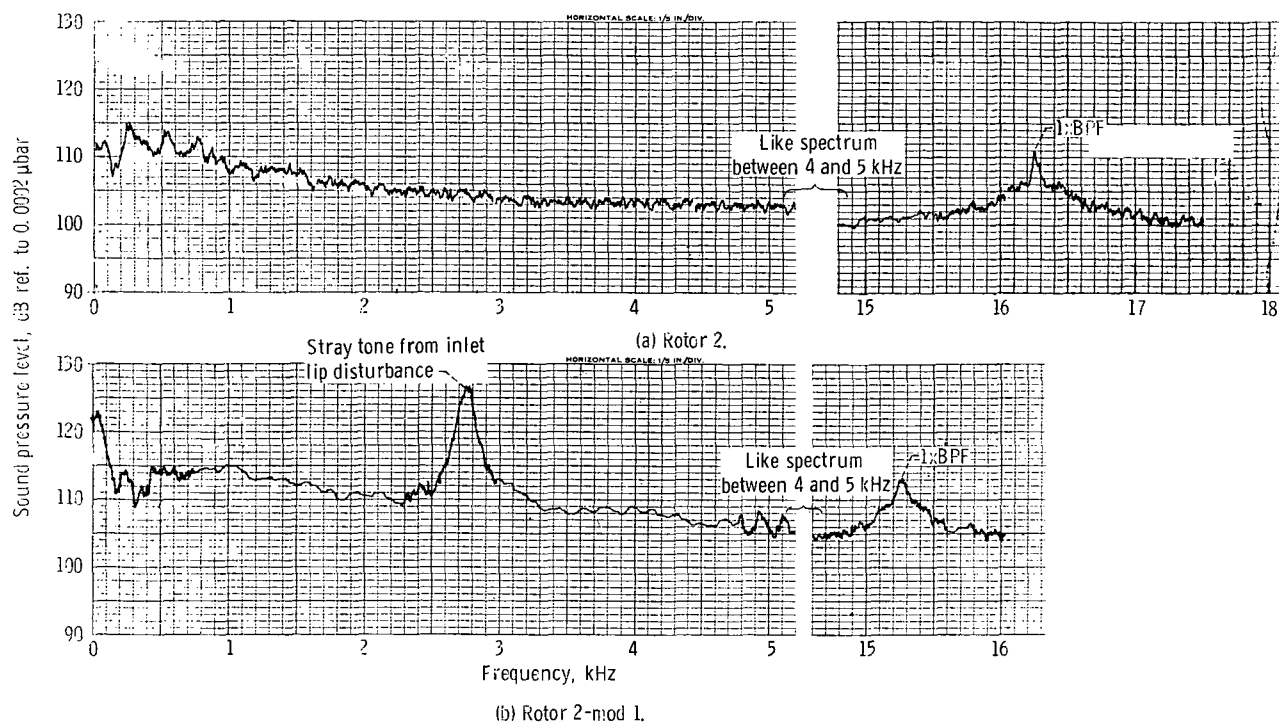

Corrected speed, $N/\sqrt{\theta}$, percent	Relative Mach number, $M'_{1,05}$	Total pressure ratio, P_2/P_1	Diffusion factor at 5-percent span, D_{05}
○ 100	1.202	1.258	0.070
	1.191	1.511	.434
	1.156	1.528	.482
□ 90	1.092	1.178	.006
	1.068	1.389	.372
	1.000	1.397	.421
◇ 80	.973	1.118	-.060
	.938	1.290	.328
	.896	1.308	.421
△ 70	.864	1.058	.112
	.818	1.213	.294
	.771	1.234	.540
▽ 60	.759	1.026	-.115
	.696	1.149	.272
	.661	1.170	.502
◠ 50	.654	1.008	-.104
	.574	1.103	.256
	.546	1.118	.543

Solid symbols denote operation near peak efficiency
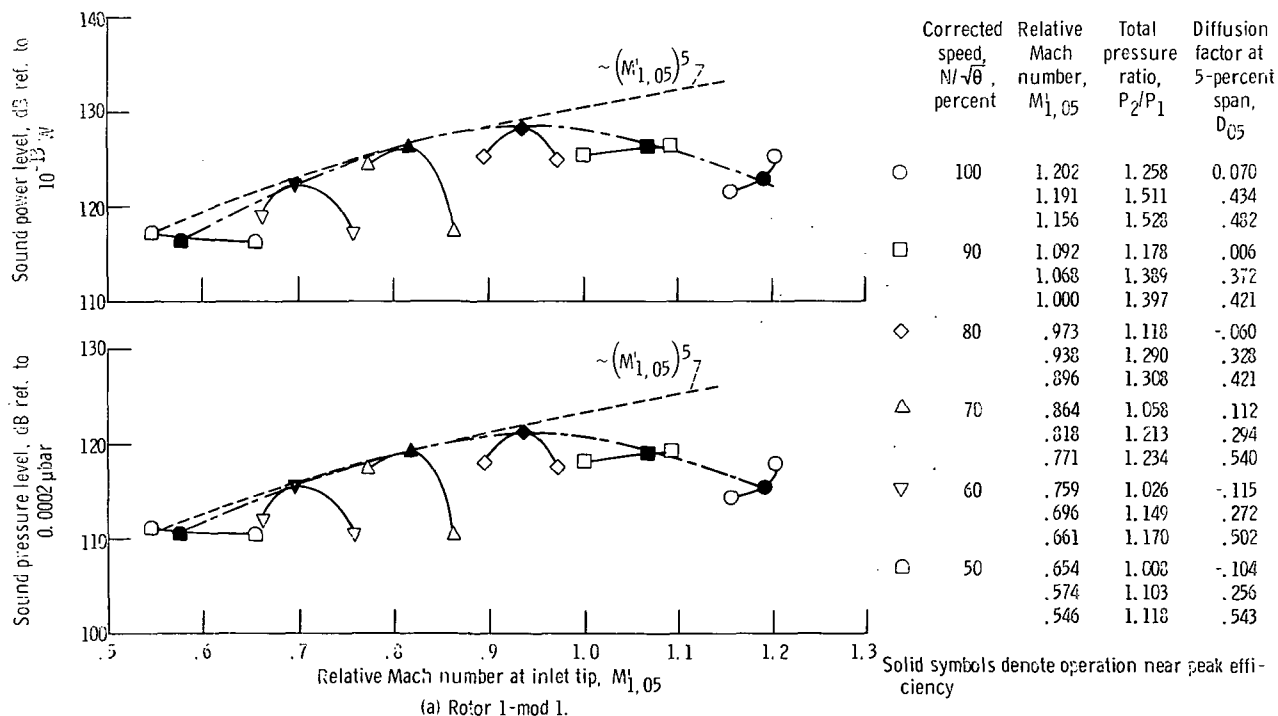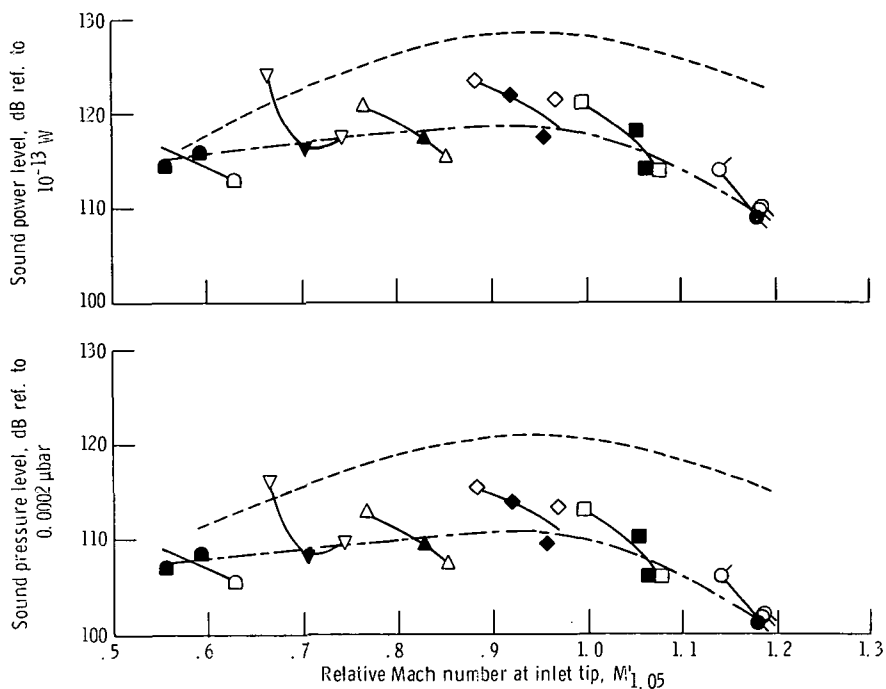
(a) Rotor 1-mod 1.

Figure 23. – Blade passing-frequency inlet sound pressure levels and sound power levels. Bandwidth, 50 hertz.
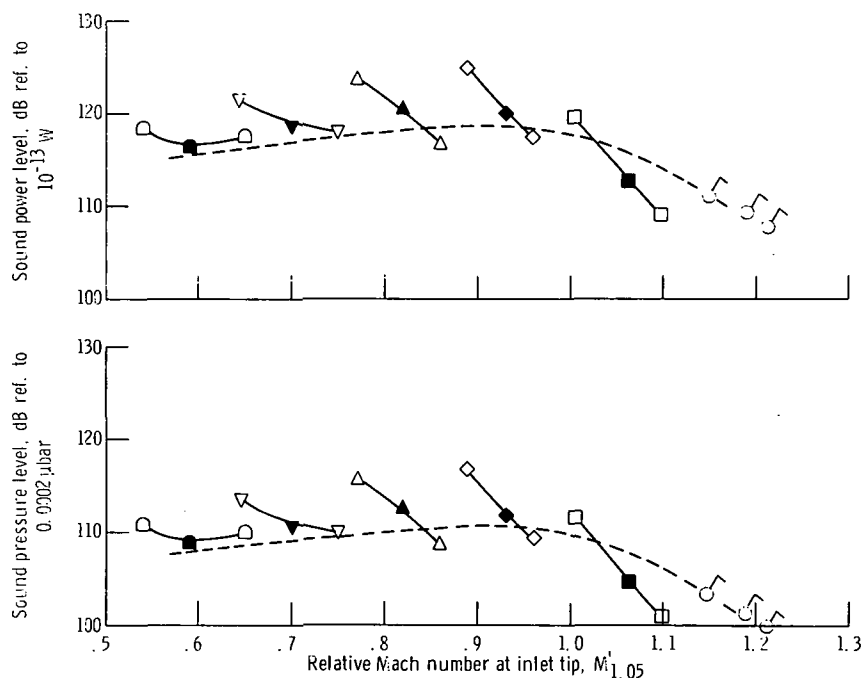
42

(b) Rotor 2.

Corrected speed, $N/\sqrt{\theta}$, percent	Relative Mach number, $M'_{1,05}$	Total pressure ratio, P_2/P_1	Diffusion factor at 5-percent span, D_{05}
O 100	1.186	1.264	0.092
	1.185	1.355	.189
	1.180	1.429	.309
	1.140	1.457	.362
□ 90	1.078	1.192	0.045
	1.062	1.325	.262
	1.052	1.358	.329
	.996	1.365	.373
◇ 80	0.969	1.119	-0.060
	.957	1.230	.201
	.920	1.265	----
	.881	1.282	.377
△ 70	0.851	1.077	-0.010
	.828	1.172	.186
	.764	1.216	.401
▽ 60	0.742	1.021	-0.106
	.705	1.115	.135
	.664	1.152	.339
◁ 50	0.628	1.028	-0.090
	.591	1.071	.060
	.557	1.106	.341

– – – – Rotor 1-mod 1 from part (a)

Solid symbols denote operation near peak efficiency

Plain symbols denote >5 dB above broadband

Tailed symbols denote <5 dB above broadband

(c) Rotor 2-mod 1.

Figure 23. – Concluded.

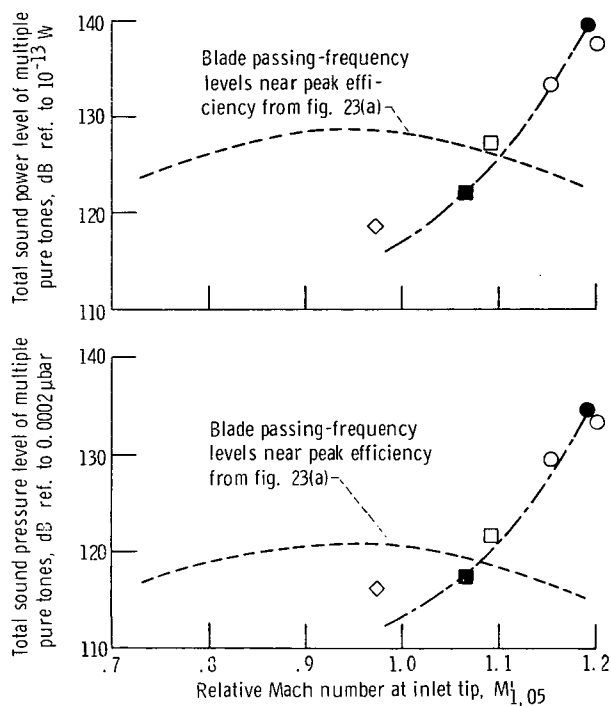| Corrected speed, $N/\sqrt{\theta}$, percent	Relative Mach number, $M'_{1,05}$	Total pressure ratio, P_2/P_1	Diffusion factor at 5-percent span, D_{05}
O 100	1.212	1.246	0.176
	1.189	1.495	.470
	1.153	1.515	.523
□ 90	1.099	1.173	0.061
	1.061	1.357	.453
	1.003	1.377	.504
◇ 80	(0.96)	(1.225)	-----
	(.93)	(1.266)	-----
	.889	1.294	0.514
△ 70	(0.86)	(1.06)	-----
	(.82)	(1.18)	-----
	(.78)	(1.22)	-----
▽ 60	(0.75)	(1.00)	-----
	(.70)	(1.12)	-----
	(.65)	(1.16)	-----
◁ 50	(0.65)	(1.00)	-----
	(.59)	(1.09)	-----
	(.54)	(1.11)	-----

– – – – Rotor 2 from part (b)

Solid symbols denote operation near peak efficiency

Plain symbols denote >5 dB above broadband

Flagged symbols denote broadband level, no apparent tones

( ) Estimated

43

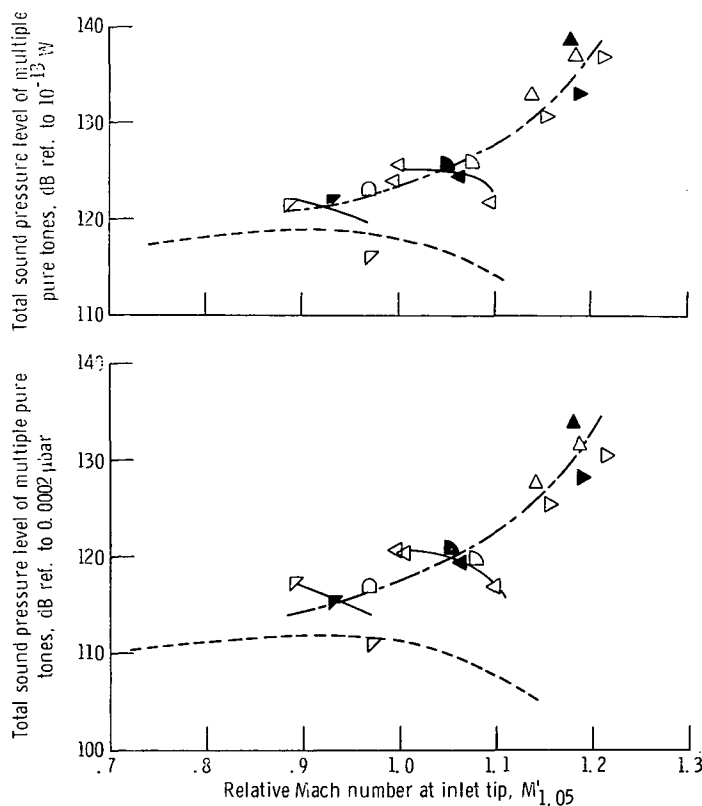| Corrected speed, $N/\sqrt{\theta}$, percent	Relative Mach number, $M'_{1,05}$	Total pressure ratio, P_2/P_1	Diffusion factor at 5-percent span, D_{05}
○ 100	1.202	1.258	0.070
	1.191	1.511	.434
	1.156	1.528	.432
□ 90	1.092	1.178	.006
	1.068	1.389	.372
◇ 80	.973	1.118	-.060

Solid symbols denote operation near peak efficiency

Blade passing-frequency levels near peak efficiency from fig. 23(a)

Blade passing-frequency levels near peak efficiency from fig. 23(a)

(a) Rotor 1-mod 1.

Figure 24. – Multiple pure-tone total inlet sound pressure levels and sound power levels. Blade passing-frequency tones not included in total. Bandwidth, 50 hertz.
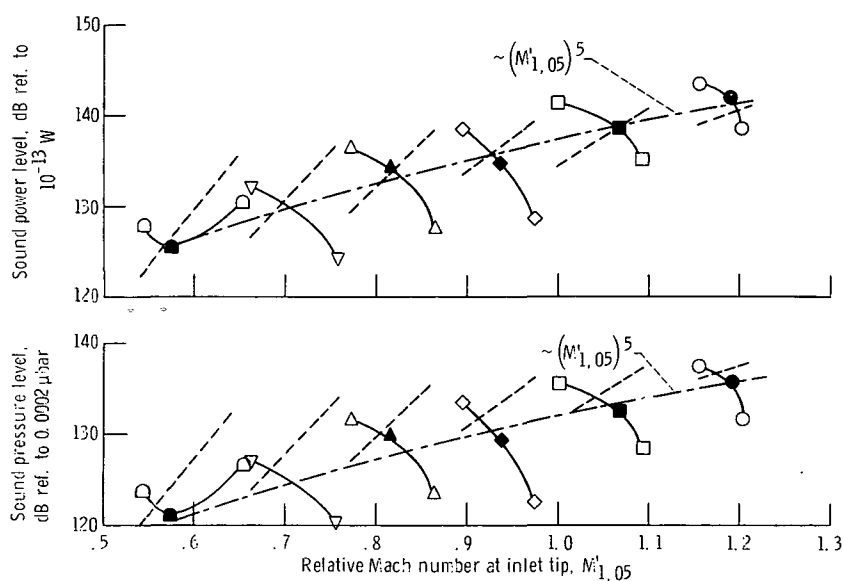
Corrected speed, $N/\sqrt{\theta}$, percent	Relative Mach number, $M'_{1,05}$	Total pressure ratio, P_2/P_1	Diffusion factor at 5-percent span, D_{05}	
△ 100	1.186	1.284	0.092	
	1.180	1.429	.309	
	1.140	1.457	.362	
◹ 90	1.078	1.192	0.045	Rotor 2
	1.052	1.358	.329	
	.996	1.365	.373	
◠ 80	0.969	1.119	-0.060	
▷ 100	1.212	1.248	0.176	
	1.189	1.495	.470	
	1.153	1.515	.523	
◁ 90	1.099	1.173	0.081	Rotor 2-mod 1
	1.061	1.397	.450	
	1.003	1.377	.504	
▽ 80	(0.96)	(1.225)	-----	
	(.93)	(1.268)	-----	
	.889	1.294	.514	

– – – – Blade passing frequency near peak efficiency from fig. 23(b) or (c)

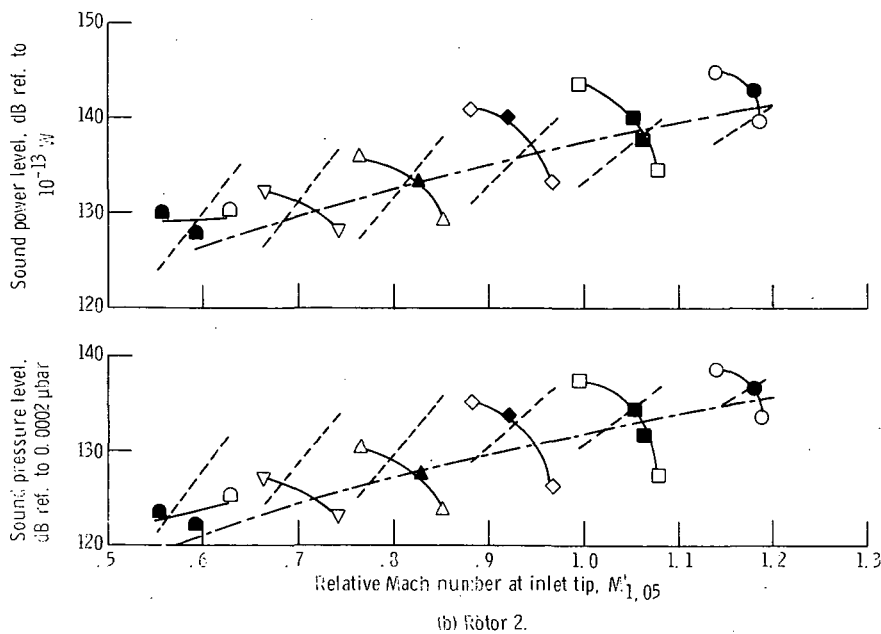Solid symbols denote operation near peak efficiency

( ) Estimated

(b) Rotor 2 and rotor 2-mod 1.

Figure 24. – Concluded.

Corrected speed, $N/\sqrt{\theta}$, percent	Relative Mach number, $M'_{1,05}$	Total pressure ratio, P_2/P_1	Diffusion factor at 5-percent span, D_{05}
○ 100	1.202	1.258	0.070
	1.191	1.511	.434
	1.156	1.528	.482
□ 90	1.092	1.179	0.006
	1.069	1.339	.372
	1.000	1.397	.421
◇ 80	0.972	1.118	-0.069
	.938	1.290	.329
	.896	1.303	.421
△ 70	0.964	1.058	0.112
	.913	1.213	.294
	.717	1.234	.540
▽ 60	0.759	1.026	-0.115
	.661	1.170	.502
◠ 50	0.654	1.008	-0.104
	.574	1.103	.256
	.546	1.118	.543

– – – – Flow noise ceiling without rotor (fig. 19(a))

Solid symbols denote operation near peak efficiency

(a) Rotor 1-mod 1.

Figure 25. – Broadband inlet sound pressure levels and sound power levels. Bandwidth, 177 to 22 400 hertz.

45

(b) Rotor 2.

Corrected speed, $N/\sqrt{\theta}$, percent	Relative Mach number, $M'_{1,05}$	Total pressure ratio, P_2/P_1	Diffusion factor at 5-percent span, D_{05}
○ 100	1.186	1.284	0.092
	1.180	1.429	.309
	1.140	1.457	.362
□ 90	1.078	1.192	0.045
	1.062	1.325	.262
	1.052	1.358	.329
	.996	1.365	.373
◇ 80	0.969	1.119	-0.060
	.920	1.265	------
	.881	1.292	.377
△ 70	0.851	1.077	-0.010
	.923	1.172	.186
	.764	1.216	.401
▽ 60	0.742	1.021	-0.106
	.705	1.115	.135
	.664	1.152	.339
◻ 50	0.628	1.028	-0.090
	.591	1.071	.080
	.557	1.108	.341

Solid symbols denote operation near peak efficiency

- - - - - Flow noise ceiling with a rotor from fig. 10(a)
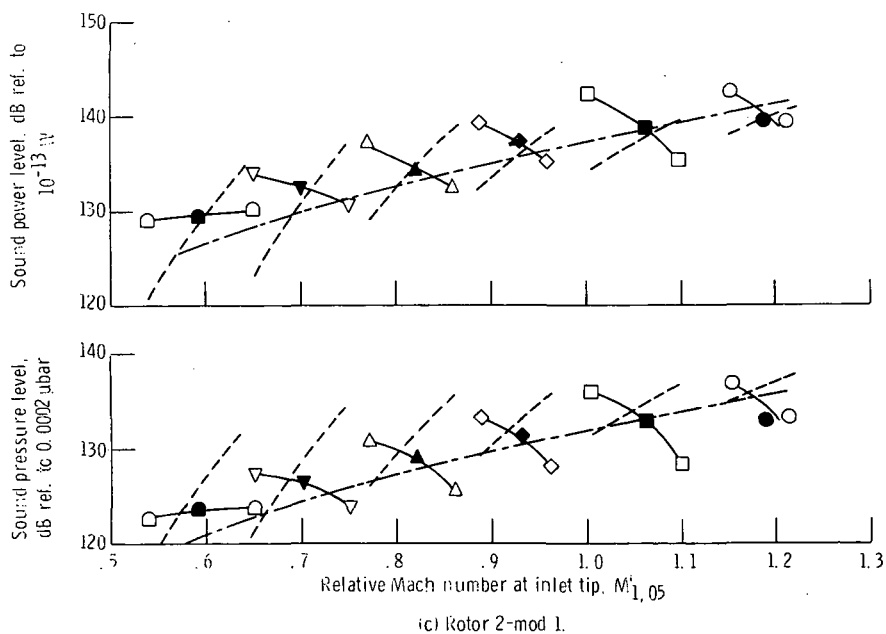
—·— Rotor 1-mod 1 from part (a)

Corrected speed, $N/\sqrt{\theta}$, percent	Relative Mach number, $M'_{1,05}$	Total pressure ratio, P_2/P_1	Diffusion factor at 5-percent span, D_{05}
○ 100	1.212	1.248	0.176
	1.189	1.495	.470
	1.153	1.515	.523
□ 90	1.099	1.173	0.081
	1.061	1.397	.450
	1.003	1.377	.504
◇ 80	(0.96)	(1.225)	-----
	(.93)	(1.263)	-----
	.889	1.294	0.514
△ 70	(0.86)	(1.06)	-----
	(.82)	(1.18)	-----
	(.73)	(1.22)	-----
▽ 60	(0.75)	(1.00)	-----
	(.70)	(1.12)	-----
	(.65)	(1.16)	-----
◻ 50	(0.65)	(1.00)	-----
	(.59)	(1.03)	-----
	(.54)	(1.11)	-----

Solid symbols denote operation near peak efficiency

( ) Estimated

- - - - Flow noise ceiling without a rotor from fig. 10(a)

—·— Rotor 1-mod 1 from part (a)

(c) Rotor 2-mod 1.

Figure 25. - Concluded.

46

"The aeronautical and space activities of the United States shall be conducted so as to contribute . . . to the expansion of human knowledge of phenomena in the atmosphere and space. The Administration shall provide for the widest practicable and appropriate dissemination of information concerning its activities and the results thereof."

—NATIONAL AERONAUTICS AND SPACE ACT OF 1958

NASA SCIENTIFIC AND TECHNICAL PUBLICATIONS

TECHNICAL REPORTS: Scientific and technical information considered important, complete, and a lasting contribution to existing knowledge.

TECHNICAL NOTES: Information less broad in scope but nevertheless of importance as a contribution to existing knowledge.

TECHNICAL MEMORANDUMS: Information receiving limited distribution because of preliminary data, security classification, or other reasons.

CONTRACTOR REPORTS: Scientific and technical information generated under a NASA contract or grant and considered an important contribution to existing knowledge.

TECHNICAL TRANSLATIONS: Information published in a foreign language considered to merit NASA distribution in English.

SPECIAL PUBLICATIONS: Information derived from or of value to NASA activities. Publications include conference proceedings, monographs, data compilations, handbooks, sourcebooks, and special bibliographies.

TECHNOLOGY UTILIZATION PUBLICATIONS: Information on technology used by NASA that may be of particular interest in commercial and other non-aerospace applications. Publications include Tech Briefs, Technology Utilization Reports and Technology Surveys.

Details on the availability of these publications may be obtained from:

SCIENTIFIC AND TECHNICAL INFORMATION OFFICE

NATIONAL AERONAUTICS AND SPACE ADMINISTRATION
Washington, D.C. 20546